Nuclear Physics with Gamma Beams at ELI-NP

P. Constantin
ELI-NP/IFIN-HH, Bucharest

EUROPEAN UNION

GUVERNUL ROMÂNIEI

Structural Instruments 2014-2020

Competitiveness Operational Programme (COP)

eli nuclear physics

Extreme Light Infrastructure - Nuclear Physics (ELI-NP) - Phase II

Project Co-financed by the European Regional Development Fund

IFIN-HH

Outline

- Gamma Beam Systems: overview
- Inverse Compton Scattering Beams
- The ELI-NP Gamma Beam System
- Nuclear Physics at ELI-NP

Gamma Rays

Gamma rays: photons with E > 100 keV (λ < 10pm)

Naturally occurring in:
- nuclear gamma radiation: E ≈ 0.1 – 10 MeV

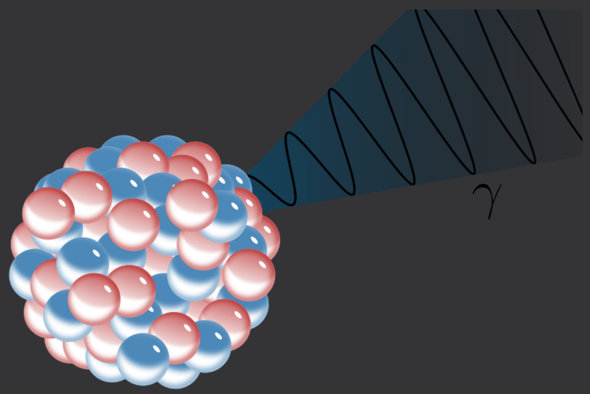

Gamma Rays

Gamma rays: photons with E > 100 keV (λ < 10pm)

Naturally occurring in:
- nuclear gamma radiation: E ≈ 0.1 – 10 MeV
- solar flares and cosmic rays (E ~ MeV)
- gamma-ray bursts (E < 10 TeV)

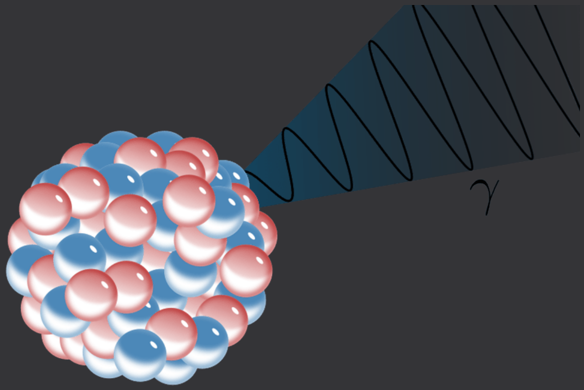

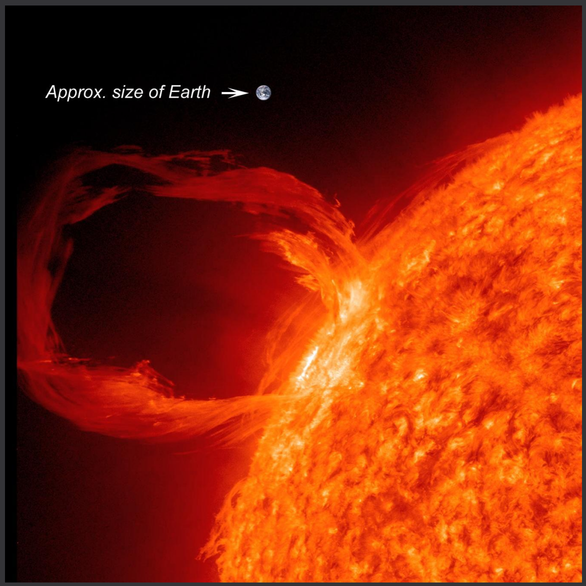

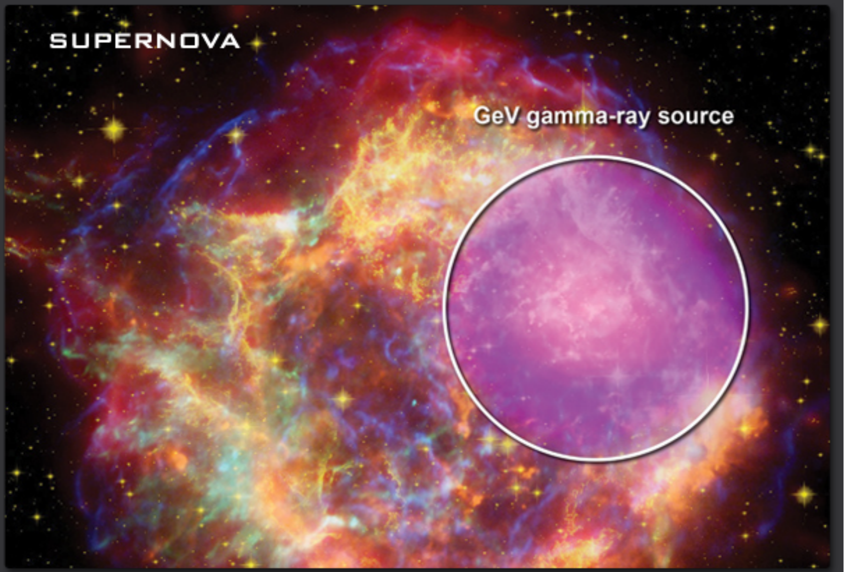

Gamma Rays

Gamma rays: photons with $E > 100$ keV ($\lambda < 10$pm)

Naturally occurring in:
- nuclear gamma radiation: $E \approx 0.1 - 10$ MeV
- solar flares and cosmic rays ($E \sim$ MeV)
- gamma-ray bursts ($E < 10$ TeV)

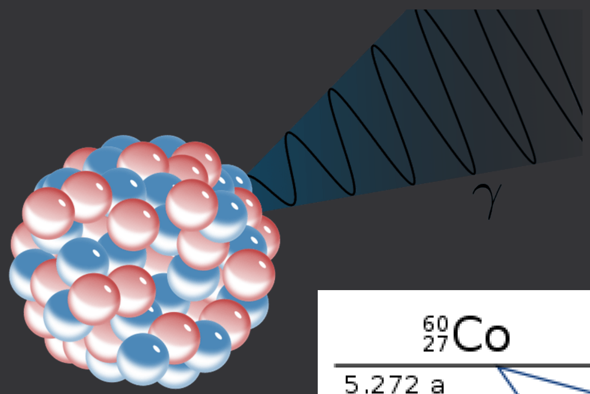

Applications:
- medicine: nuclear imaging (^{99m}Tc in SPECT, ^{22}Na in PET), cancer treatment
- gamma-ray irradiators (^{60}Co): sterilization of food and medical products, photo-polymerization of chemical compounds
- gamma imaging sensors in many industries (^{60}Co, ^{137}Cs): mining, chemical, agriculture, etc.
- material science
- the only way to turn physicists into superheroes

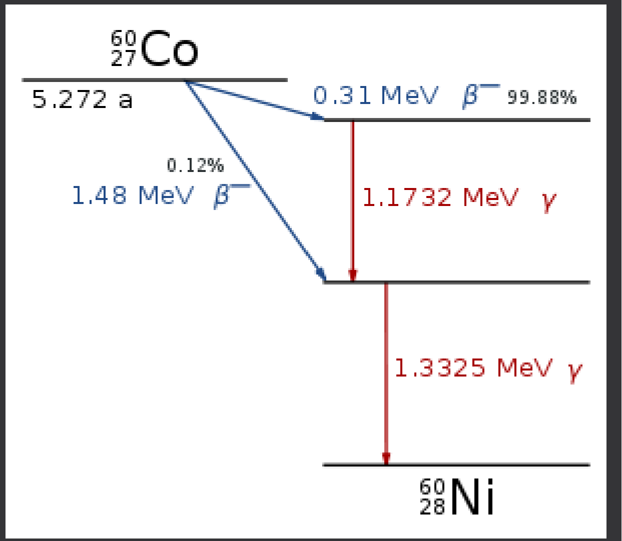

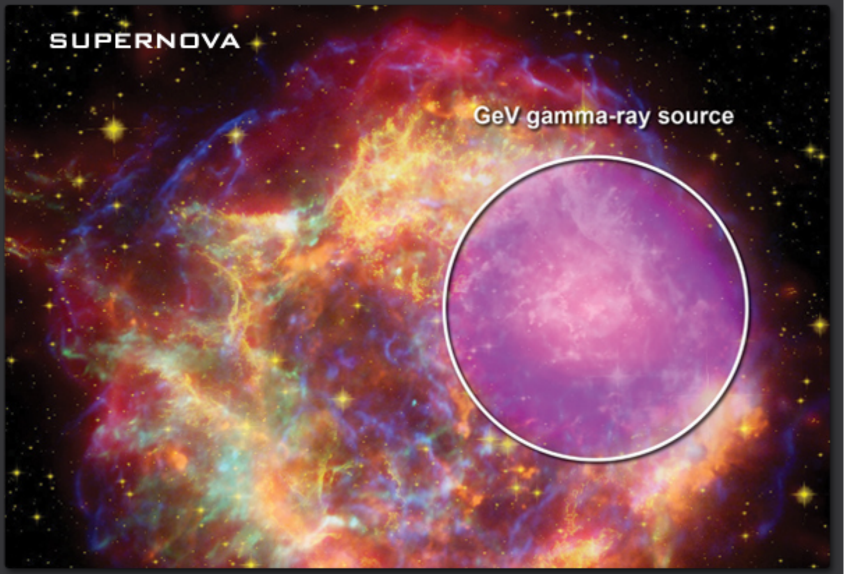

Gamma Rays

Gamma rays: photons with E > 100 keV (λ < 10pm)

Naturally occurring in:
- nuclear gamma radiation: E ≈ 0.1 – 10 MeV
- solar flares and cosmic rays (E ~ MeV)
- gamma-ray bursts (E < 10 TeV)

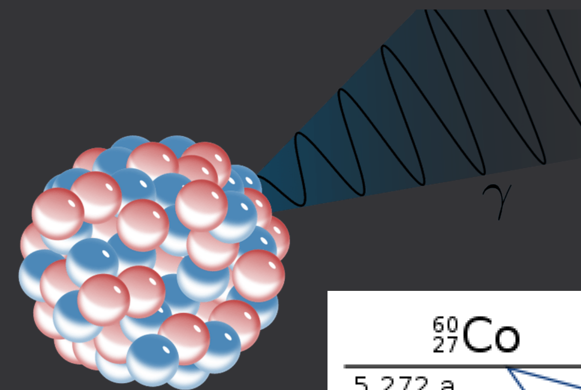

Applications:
- medicine: nuclear imaging (^{99m}Tc in SPECT, ^{22}Na in PET), cancer treatment
- gamma-ray irradiators (^{60}Co): sterilization of food and medical products, photo-polymerization of chemical compounds
- gamma imaging sensors in many industries (^{60}Co, ^{137}Cs): mining, chemical, agriculture, et
- material science
- the only way to make s

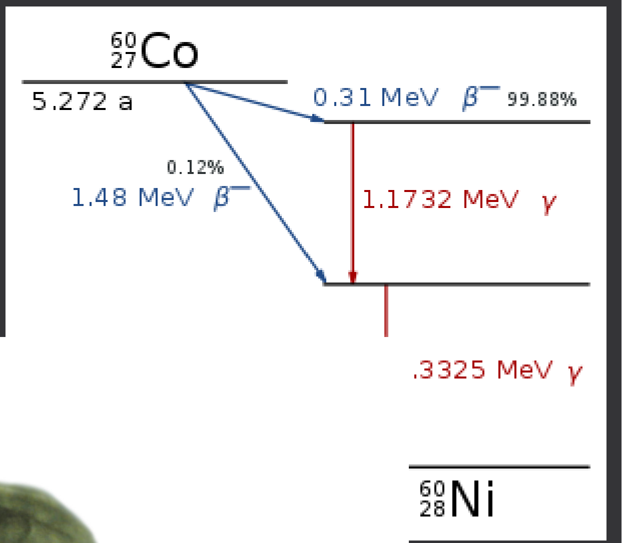

Gamma Beam Systems

Goals:

- small divergence $\Delta\theta$ (strong forward focusing)
- variable energy E (5–20 MeV) with low bandwidth (energy resolution) $BW = \Delta E / E$
- high brilliance B
- high polarization (linear/circular) desirable

$$B \equiv \frac{photons}{s \cdot mrad^2 \cdot mm^2 \cdot 0.1\,\%BW}$$

Number of emitted gammas per second, unit of solid angle and transversal size within 0.1% of energy

Gamma Beam Systems

Goals:

- small divergence $\Delta\theta$ (strong forward focusing)
- variable energy E (5–20 MeV) with low bandwidth (energy resolution) $BW = \Delta E/E$
- high brilliance B
- high polarization (linear/circular) desirable

$$B \equiv \frac{photons}{s \cdot mrad^2 \cdot mm^2 \cdot 0.1\,\% BW}$$

Number of emitted gammas per second, unit of solid angle and transversal size within 0.1% of energy

Candidate sources:

1) radioactive sources: γ emitters (^{60}Co) or β^+ emitters (^{22}Na)
2) nuclear reactions: (n,γ), (p,γ), etc.
3) electron bremsstrahlung
4) photon tagging electron bremsstrahlung
5) positron annihilation in-flight
6) Coulomb excitation
7) inverse Compton scattering

Gamma Beam Systems

Goals:
- small divergence $\Delta\theta$ (strong forward focusing)
- variable energy E (5–20 MeV) with low bandwidth (energy resolution) $BW=\Delta E/E$
- high brilliance B
- high polarization (linear/circular) desirable

$$B \equiv \frac{photons}{s \cdot mrad^2 \cdot mm^2 \cdot 0.1\,\%BW}$$

Number of emitted gammas per second, unit of solid angle and transversal size within 0.1% of energy

Candidate sources:
1) radioactive sources: γ emitters (^{60}Co) or β^+ emitters (^{22}Na)
2) nuclear reactions: (n,γ), (p,γ), etc.
3) electron bremsstrahlung
4) photon tagging electron bremsstrahlung
5) positron annihilation in-flight
6) Coulomb excitation
7) inverse Compton scattering

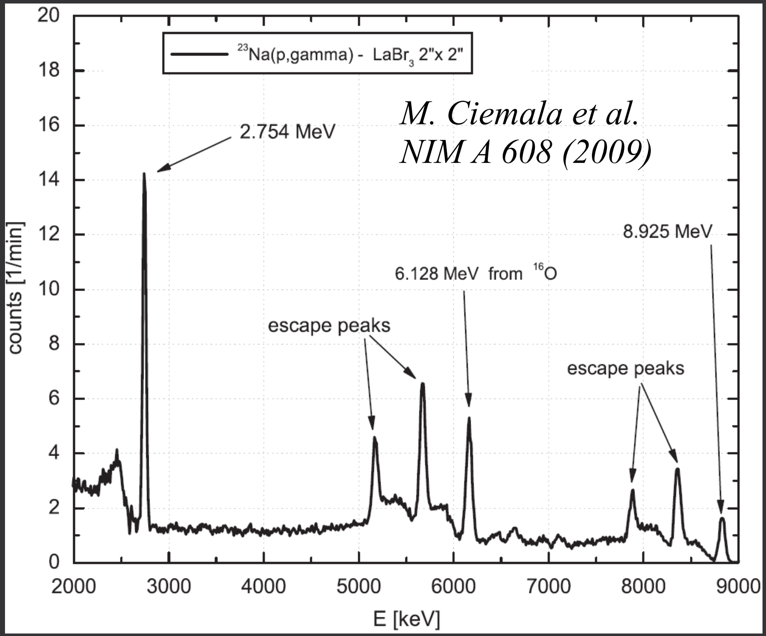

Spectrum of $^{23}Na(p,\gamma)^{24}Mg$ at E_r=1.318MeV (Q=11.69MeV)

Gamma Beam Systems:
Electron Bremsstrahlung (I)

Bremsstrahlung ("braking radiation") = electromagnetic radiation of a charged particle decelerated by another charged particle.

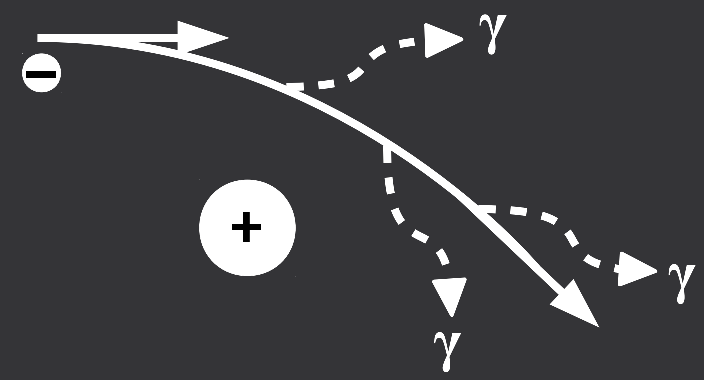

Gamma Beam Systems: Electron Bremsstrahlung (I)

Bremsstrahlung ("braking radiation") = electromagnetic radiation of a charged particle decelerated by another charged particle.

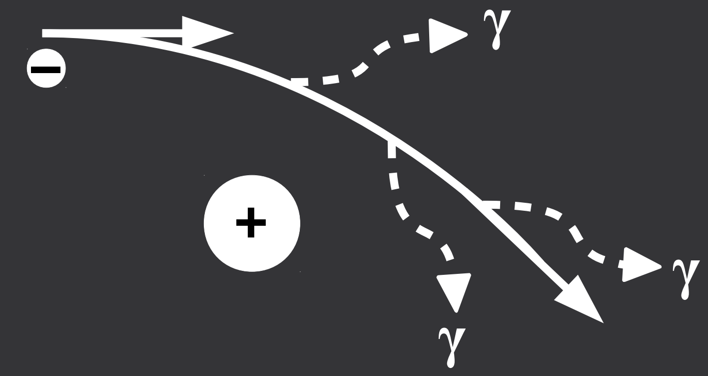

Classical electrodynamics radiated energy: $S(E) \sim a^2$
Charge in Coulomb field: $F_C \sim -qZ/r^2 = ma \rightarrow \mathbf{S \sim Z^2/m^2}$
Strongest radiation: **electron beams in high-Z matter**

Gamma Beam Systems: Electron Bremsstrahlung (I)

Bremsstrahlung ("braking radiation") = electromagnetic radiation of a charged particle decelerated by another charged particle.

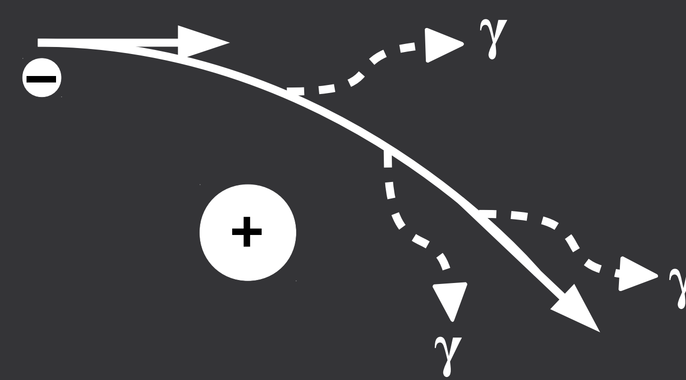

Classical electrodynamics radiated energy: $S(E) \sim a^2$

Charge in Coulomb field: $F_C \sim -qZ/r^2 = ma \rightarrow \mathbf{S \sim Z^2/m^2}$

Strongest radiation: **electron beams in high-Z matter**

$E > E_c \approx 700\,\text{MeV}/Z$ electrons lose energy mainly by bremsstrahlung

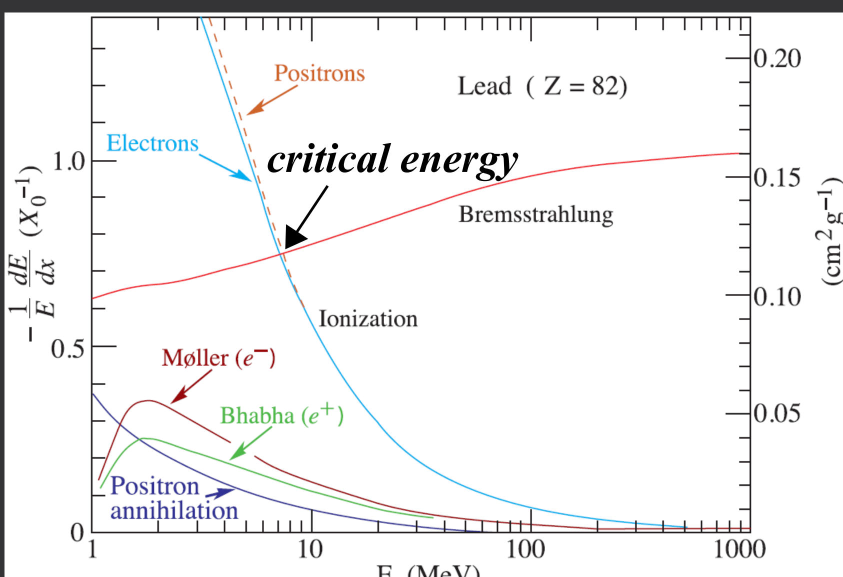

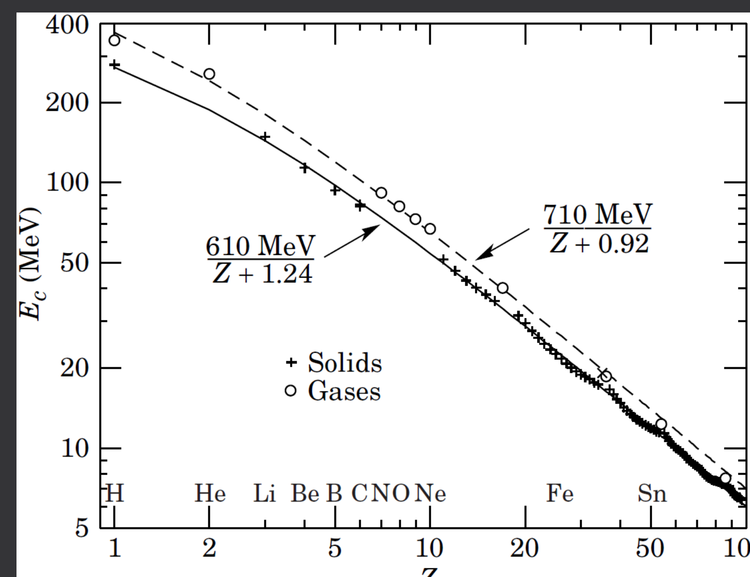

e^-/e^+ fractional energy loss per radiation length

Gamma Beam Systems:
Electron Bremsstrahlung (II)

Bethe-Heitler cross-section:
- high electron energy E_{kin} approximation:

$$\frac{d\sigma}{dy} \approx \frac{A}{X_0 N_A E_{kin}} \left(\frac{4}{3y} - \frac{4}{3} + y \right) \qquad y \equiv \frac{E_\gamma}{E_{kin}} = \frac{\hbar\omega}{E_{kin}}$$

R. Schwengner et al., NIM A 555 (2005)

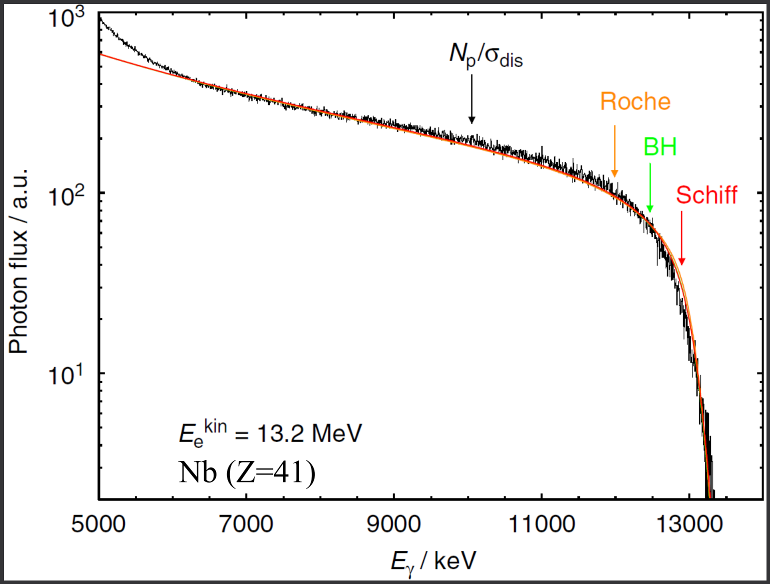

Gamma Beam Systems: Electron Bremsstrahlung (II)

Bethe-Heitler cross-section:
- high electron energy E_{kin} approximation:

$$\frac{d\sigma}{dy} \approx \frac{A}{X_0 N_A E_{kin}} \left(\frac{4}{3y} - \frac{4}{3} + y \right) \qquad y \equiv \frac{E_\gamma}{E_{kin}} = \frac{\hbar\omega}{E_{kin}}$$

→ far from high resolution (monochromatic) spectrum

→ large background from low energy gammas $\sim 1/E_\gamma$

R. Schwengner et al., NIM A 555 (2005)

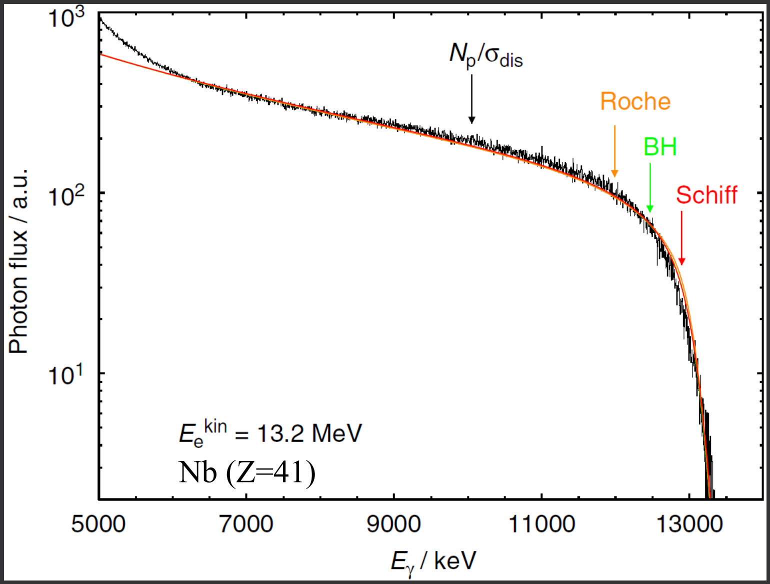

Gamma Beam Systems: Electron Bremsstrahlung (II)

Bethe-Heitler cross-section:
- high electron energy E_{kin} approximation:

$$\frac{d\sigma}{dy} \approx \frac{A}{X_0 N_A E_{kin}} \left(\frac{4}{3y} - \frac{4}{3} + y \right) \qquad y \equiv \frac{E_\gamma}{E_{kin}} = \frac{\hbar\omega}{E_{kin}}$$

→ far from high resolution (monochromatic) spectrum

→ large background from low energy gammas $\sim 1/E_\gamma$

→ weak forward focusing

→ no (E_γ, θ) correlation: no improvement by collimation

R. Schwengner et al., NIM A 555 (2005)

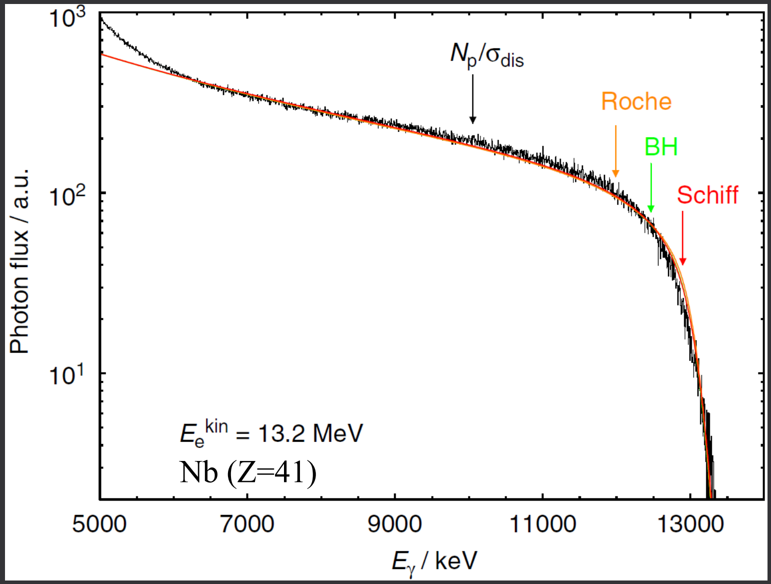

C. Köhn, U. Ebert, Atmos.Res. 135 (2014)

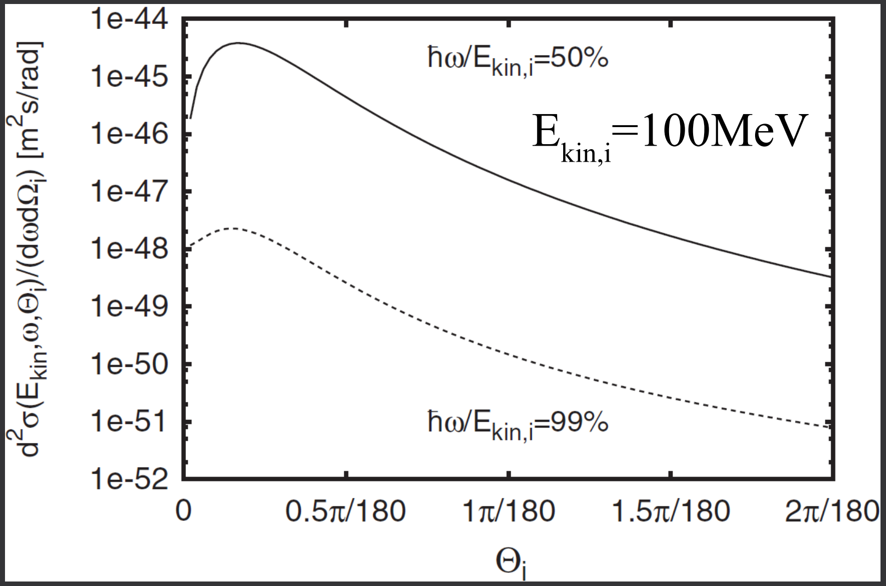

Gamma Beam Systems: Electron Bremsstrahlung (II)

Bethe-Heitler cross-section:
- high electron energy E_{kin} approximation:

$$\frac{d\sigma}{dy} \approx \frac{A}{X_0 N_A E_{kin}} \left(\frac{4}{3y} - \frac{4}{3} + y \right) \qquad y \equiv \frac{E_\gamma}{E_{kin}} = \frac{\hbar\omega}{E_{kin}}$$

→ far from high resolution (monochromatic) spectrum

→ large background from low energy gammas $\sim 1/E_\gamma$

→ weak forward focusing

→ no (E_γ,θ) correlation: no improvement by collimation

→ small degree of linear polarization

relativistic electrons: peak γ linear pol. at $\theta_{peak} \approx m_e c^2/E_e$

R. Schwengner et al., NIM A 555 (2005)

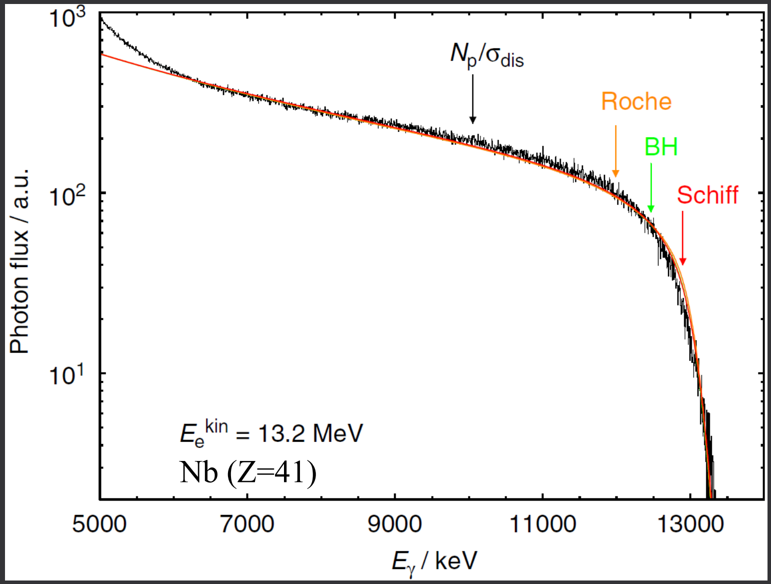

J.W. Motz, R.C. Placious, Nuovo Cimento 15 (1960) 571

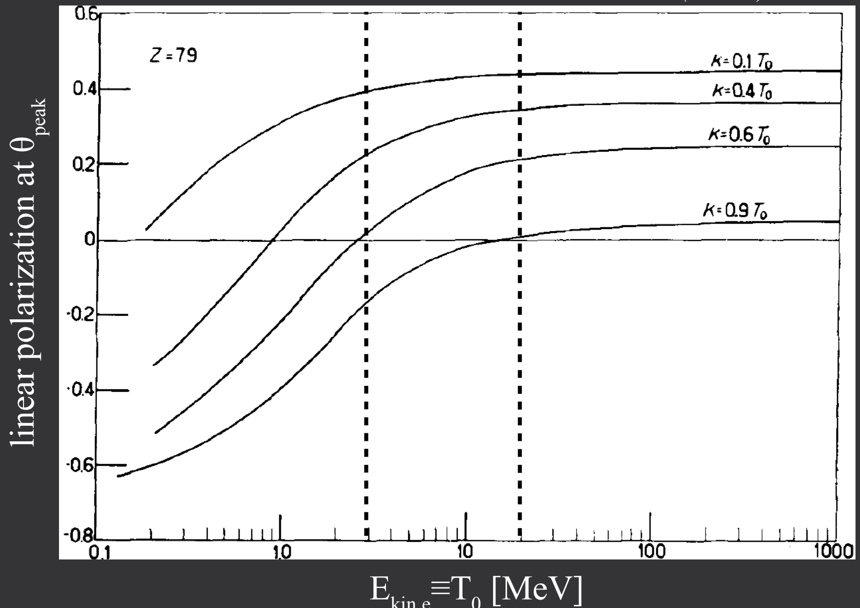

C. Köhn, U. Ebert, Atmos.Res. 135 (2014)

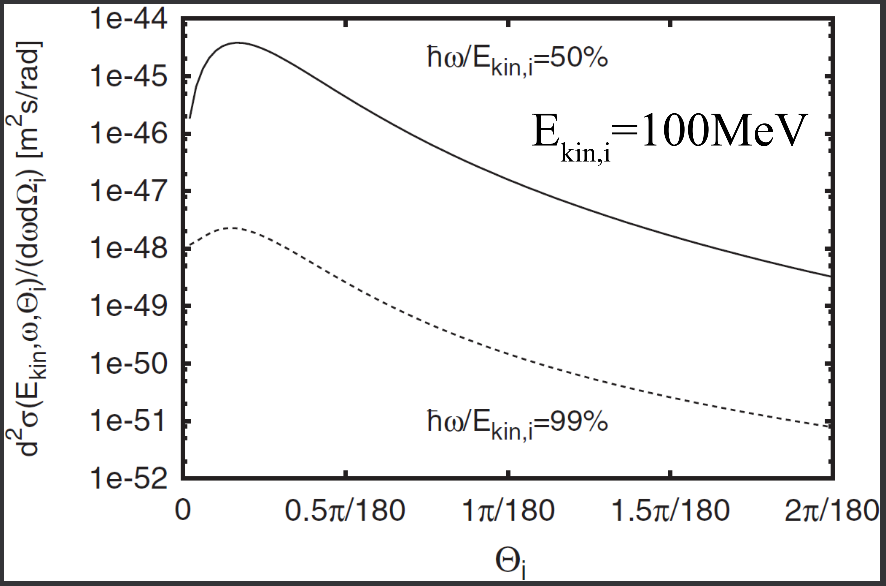

Gamma Beam Systems: Electron Bremsstrahlung (III)

Spectra measured with bremsstrahlung gamma systems need to be deconvoluted:

$$Y(E_m) = \int_{E_{th}}^{E_m} W(E_m, E)\,\sigma(E)\,dE$$

E_m = end-point energy
$Y(E_m)$ = measured yield
$W(E_m,E)$ = bremsstrahlung spectrum
$\sigma(E)$ = reaction cross-section

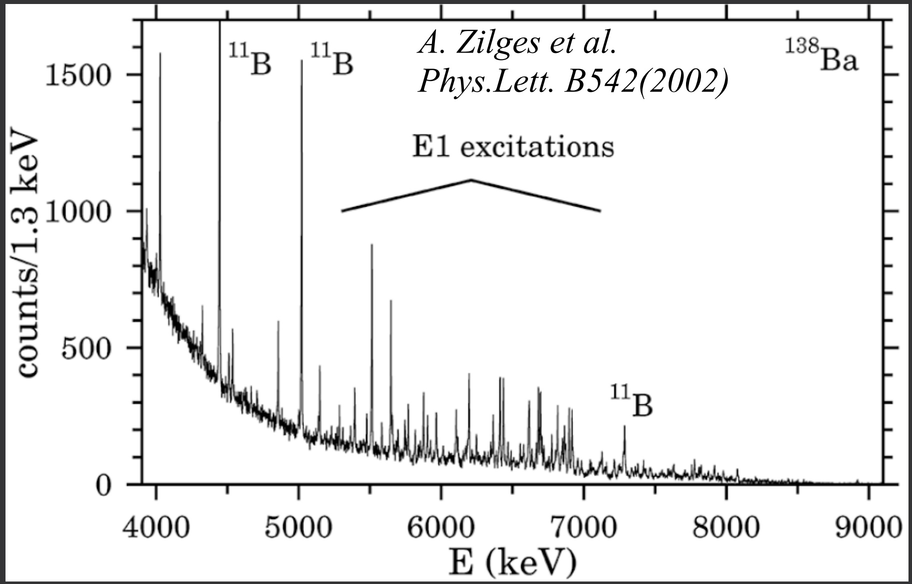

^{138}Ba(γ,γ') spectrum: E1 transitions from $J^{\pi}=1^{-}$ to g.s.

Gamma Beam Systems: Electron Bremsstrahlung (III)

Spectra measured with bremsstrahlung gamma systems need to be deconvoluted:

$$Y(E_m) = \int_{E_{th}}^{E_m} W(E_m, E)\,\sigma(E)\,dE$$

E_m = end-point energy
$Y(E_m)$ = measured yield
$W(E_m,E)$ = bremsstrahlung spectrum
$\sigma(E)$ = reaction cross-section

→ energy resolutions ~ 200keV

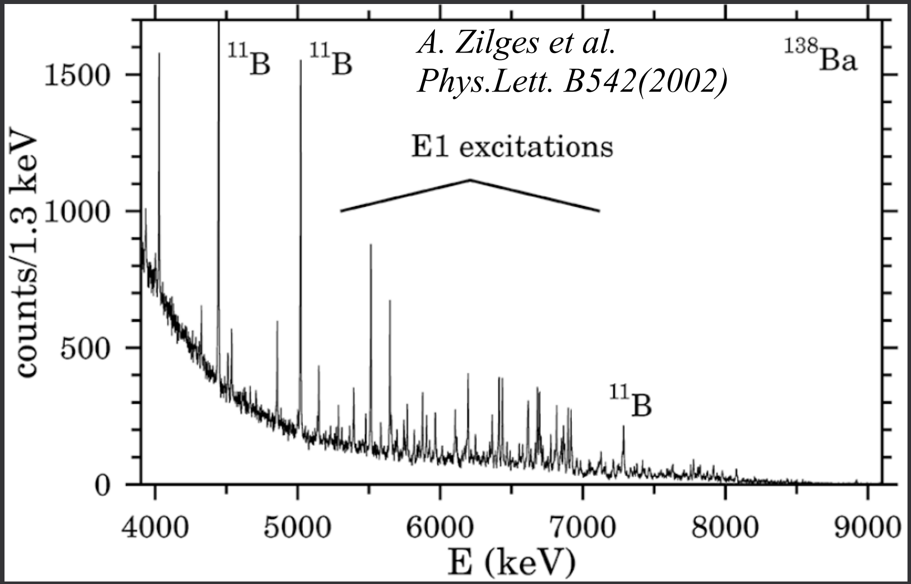

^{138}Ba(γ,γ') spectrum: E1 transitions from $J^{\pi}=1^{-}$ to g.s.

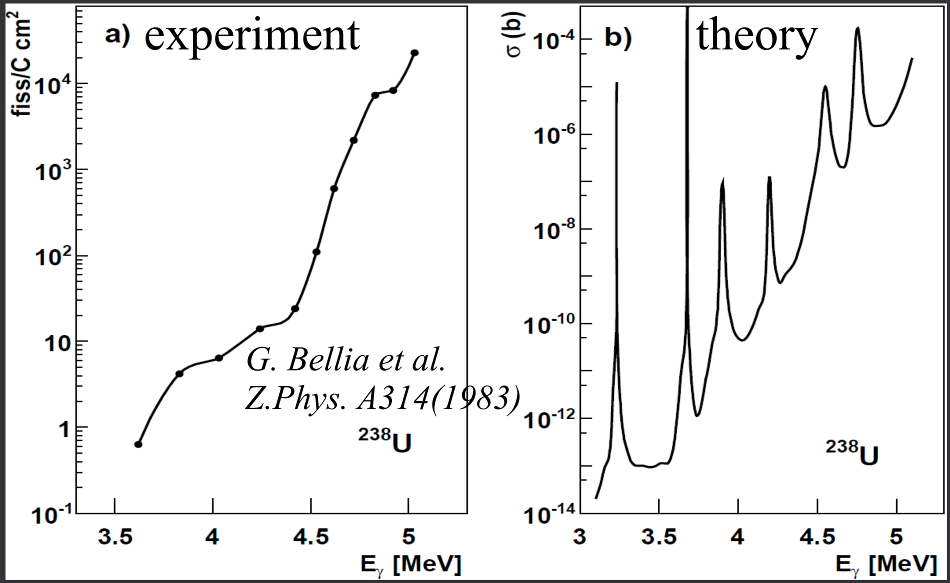

^{238}U photofission: experiment vs. theory

Gamma Beam Systems:
Electron Bremsstrahlung (IV)

ELBE (Electron Linear accelerator of high Brilliance and low Emittance), Germany

R. Schwengner et al., NIM A 555 (2005)

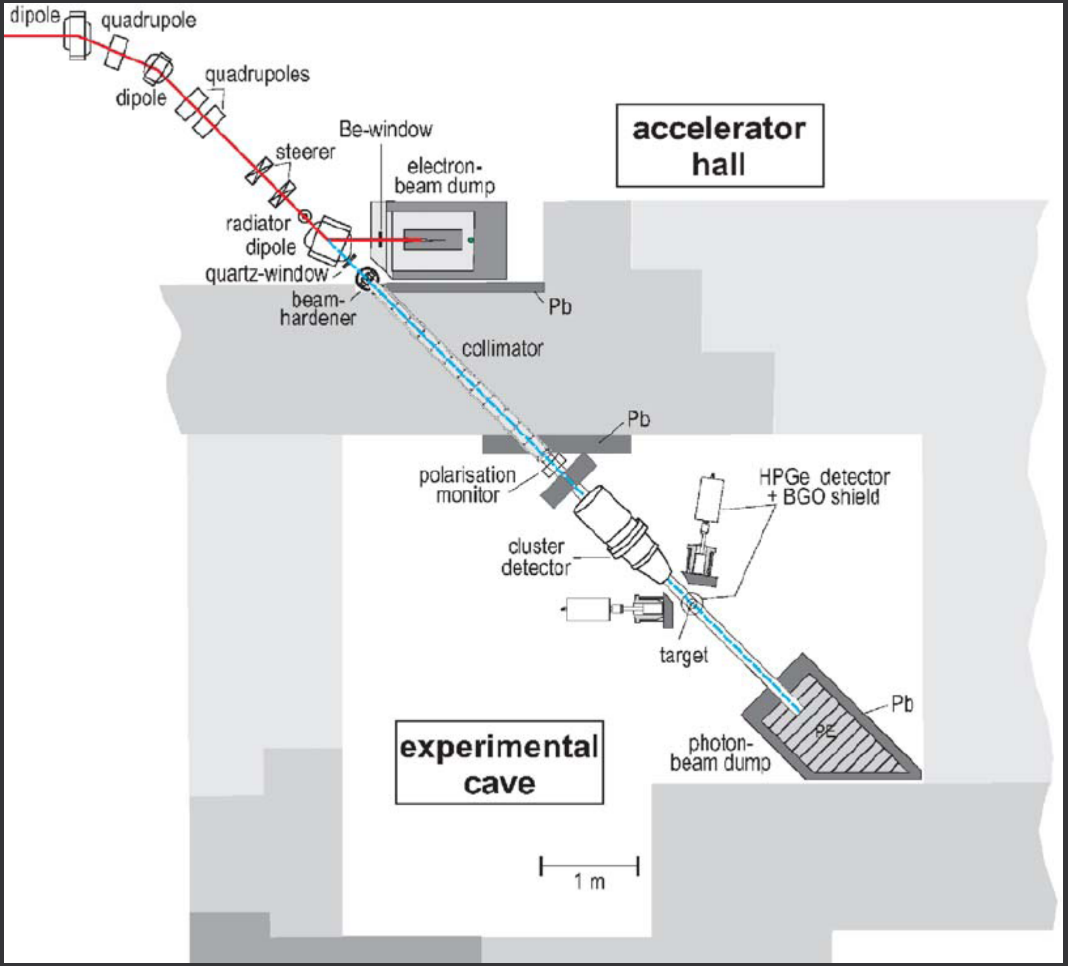

Gamma Beam Systems: Electron Bremsstrahlung (IV)

ELBE (Electron Linear accelerator of high Brilliance and low Emittance), Germany

R. Schwengner et al., NIM A 555 (2005)

Electron beam:
E_{max}=20MeV, I_{max}=1mA

Gamma beam:
Intensity ~ 10^{10} γ/s/keV/cm^2
Divergence ~ 5 mrad after colimator
Linear polarization ~ 5-25%

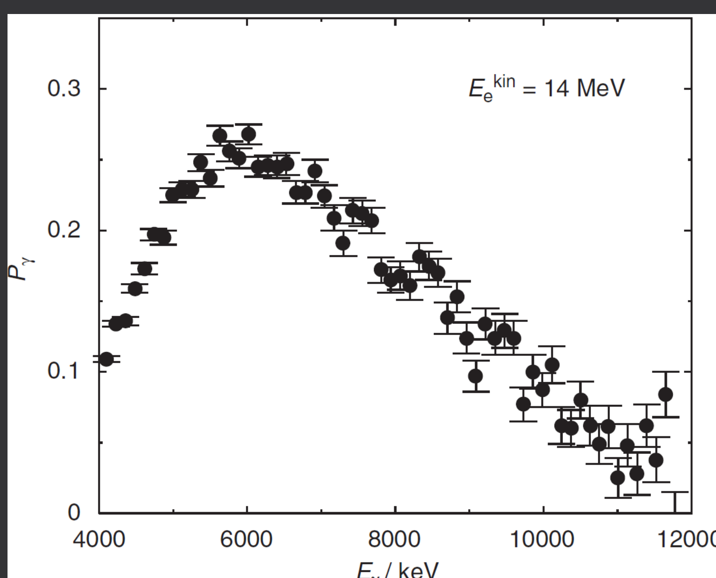

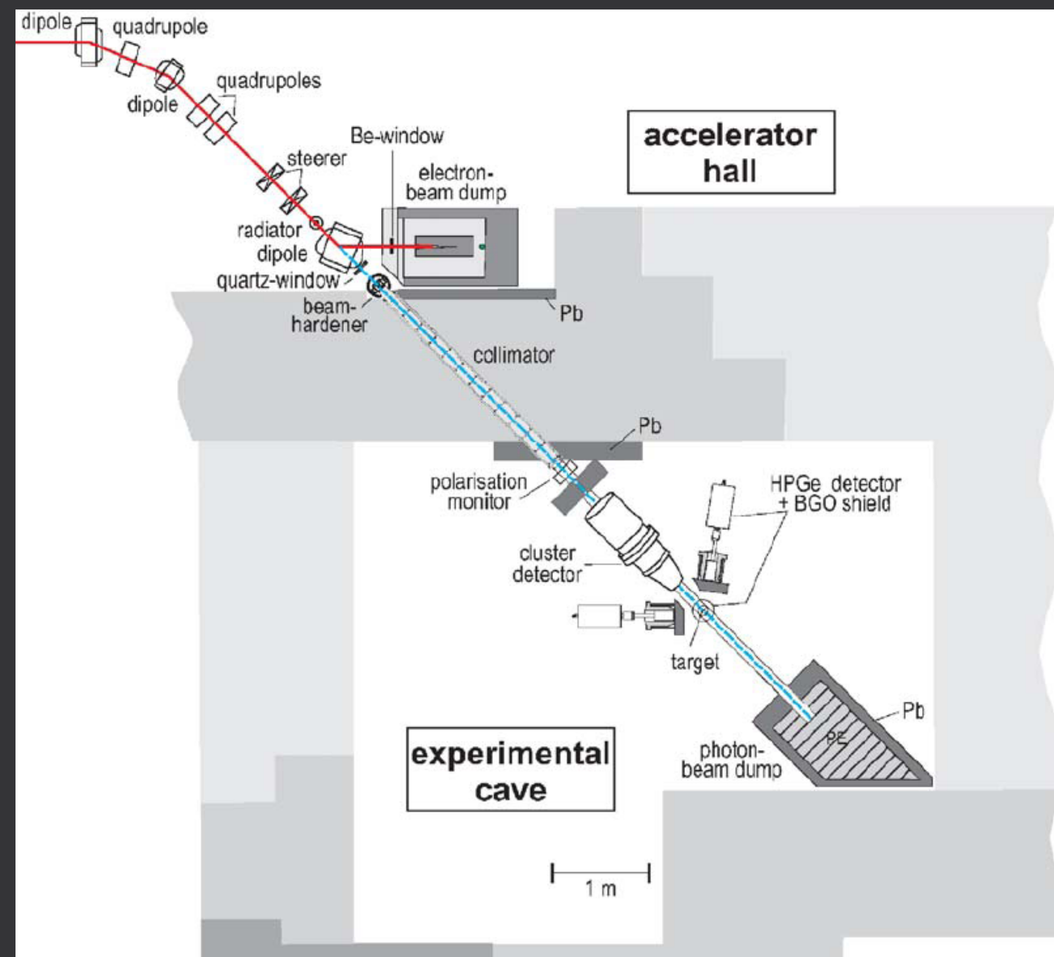

Gamma Beam Systems: Electron Bremsstrahlung (V)

DHIPS (Darmstadt High Intensity Photon Setup) @ **S-DANILAC**
(Superconducting Darmstadt electron LINear ACcelerator)

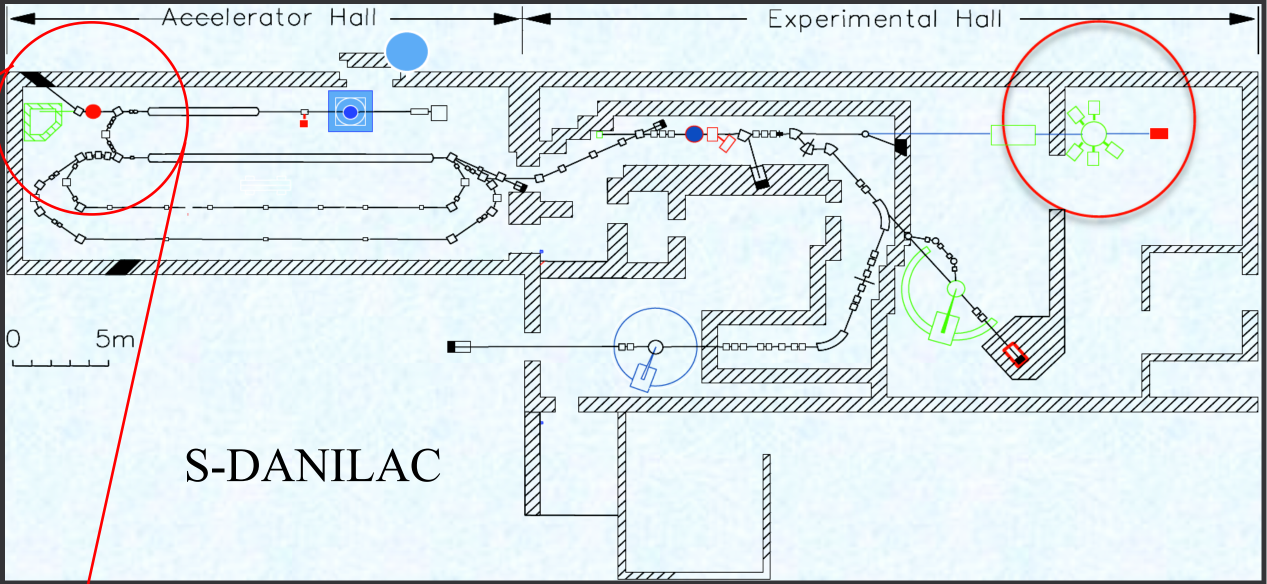

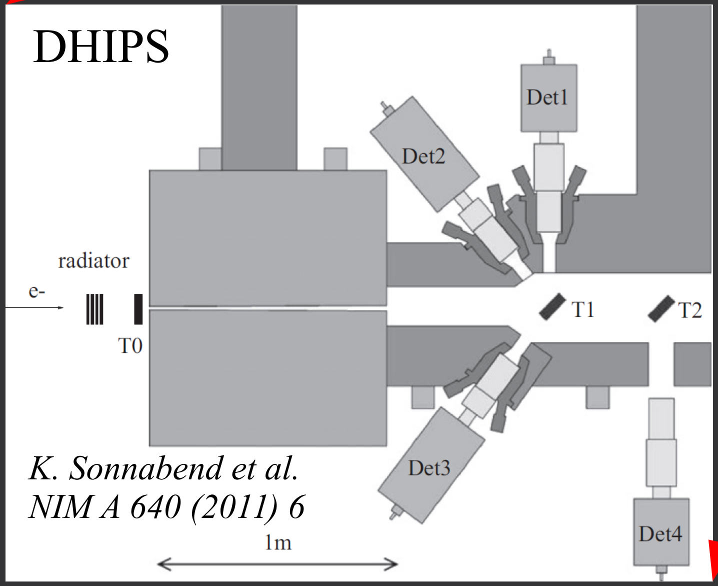

Electron beam:
E_{max}=10-130MeV, I_{max}=60µA

Gamma beam:
Maximum energy = 10 MeV
Intensity: $T_0=3\cdot10^8$ γ/s/keV/cm², $T_1=10^6$ γ/s/keV/cm²

Gamma Beam Systems: Photon Tagging

1) bremsstrahlung with thin radiator/convertor
   → at most $1\gamma/e^-$
2) measure energy of scattered e^- with
   → zero degree spectrometer
3) $\gamma - e^-$ coincidence: $E_\gamma = E_0 - E_e$
   (E_γ measured event-by-event)

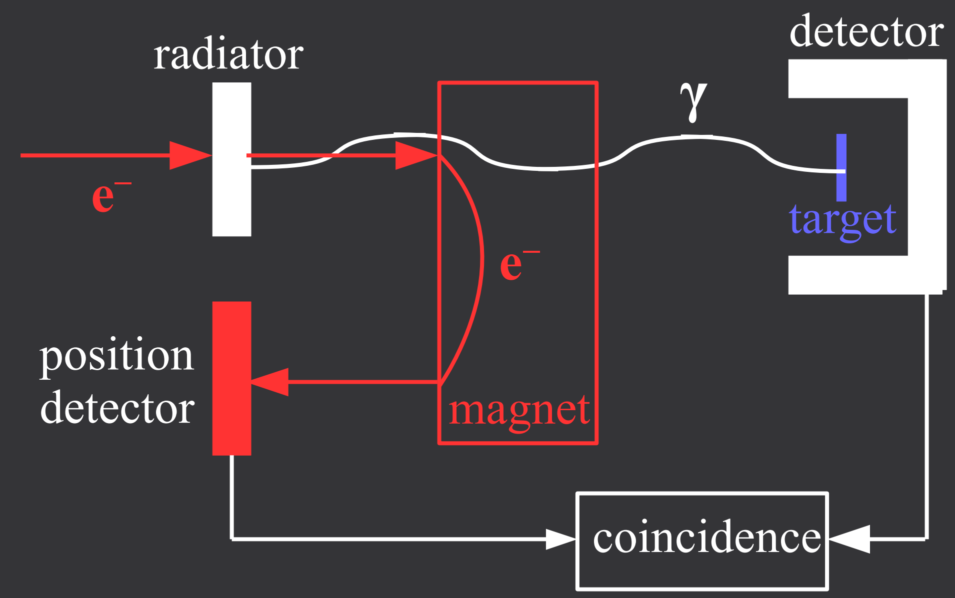

Gamma Beam Systems: Photon Tagging

1) bremsstrahlung with thin radiator/convertor
→ at most 1γ/e⁻

2) measure energy of scattered e⁻ with
→ zero degree spectrometer

3) γ – e⁻ coincidence: $E_\gamma = E_0 - E_e$
(E_γ measured event-by-event)

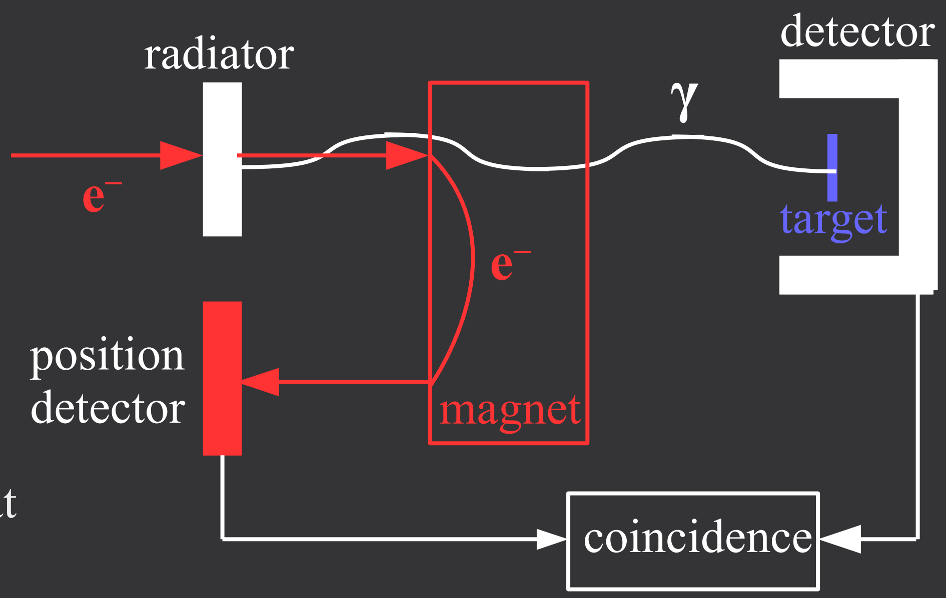

NEPTUN @ S-DANILAC:
– E_γ=6–20MeV
– high energy resolution: ΔE_γ=35keV (ΔE_e=25keV) at E_γ=10MeV
– low gamma intensity: $5\cdot10^4$ γ/s/keV (low primary beam intensity, large coincidence time window ~ 2μs)
– final γ spectrum has the same bremsstrahlung shape

NEPTUN @ S-DANILAC

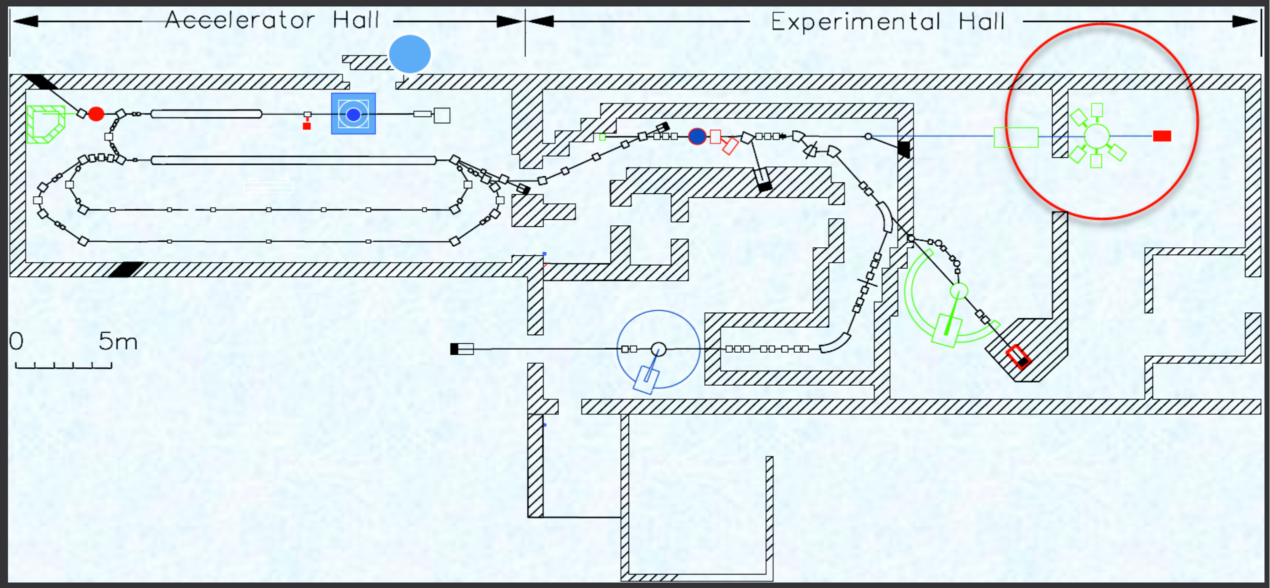

Gamma Beam Systems:
Positron In-flight Annihilation (I)

Gamma produced by **annihilation** of a relativistic positron ($\gamma=E_p/m>>1$) on an electron at rest ($E_e=m$):

$$E_\gamma(\theta_\gamma)=\frac{m}{1-\frac{p_p}{E_p+m}\cos(\theta_\gamma)}$$

$E_p=9.5$MeV: $\theta_\gamma<0.15$rad → $E_\gamma=8\text{-}10$MeV

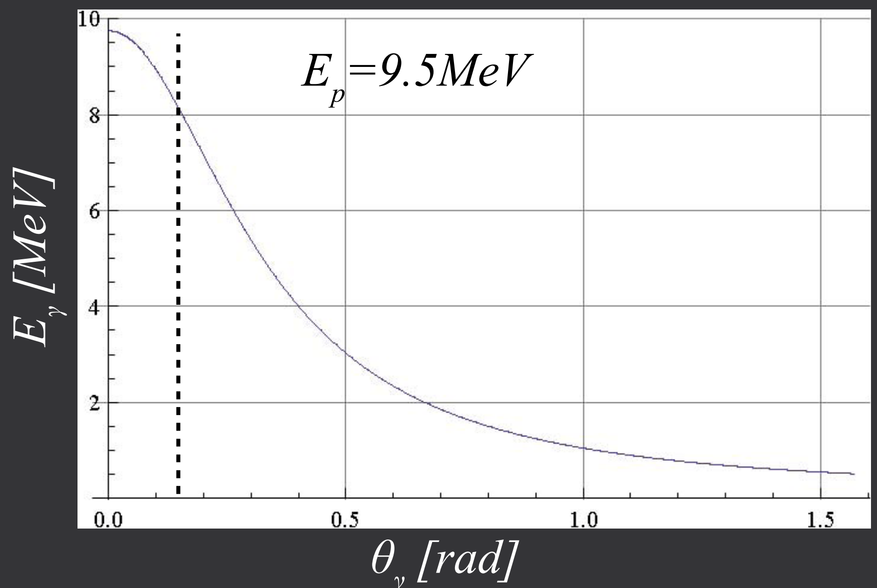

Gamma Beam Systems:
Positron In-flight Annihilation (I)

Gamma produced by **annihilation** of a relativistic positron ($\gamma=E_p/m>>1$) on an electron at rest ($E_e=m$):

- (E_γ,θ_γ) correlation: hardening by collimation
- focused forward in cone $\Delta\theta\approx1/\gamma$: small divergence
- energy range $\Delta E\approx E_{\gamma,max}/2\gamma$: good resolution

$$E_\gamma(\theta_\gamma)=\frac{m}{1-\frac{p_p}{E_p+m}\cos(\theta_\gamma)}$$

E_p=9.5MeV: θ_γ<0.15rad → E_γ=8-10MeV

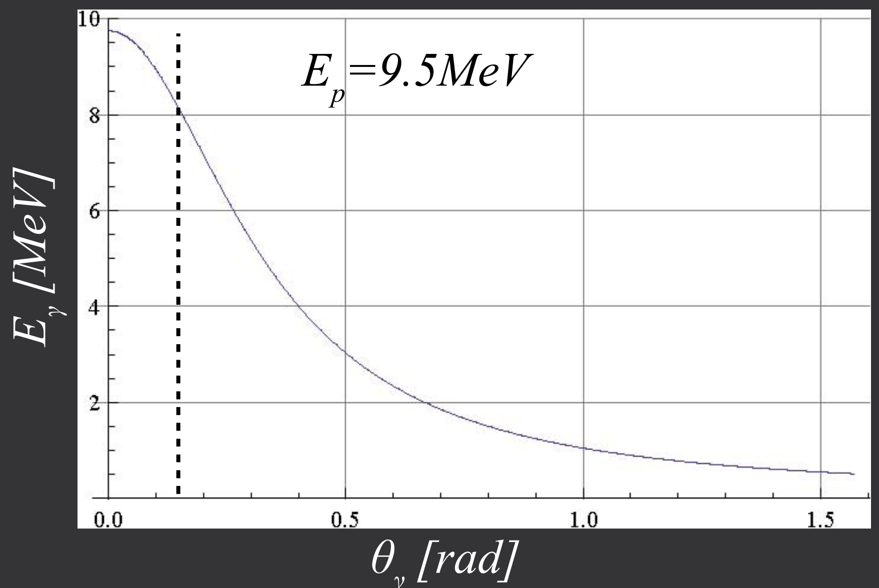

Gamma Beam Systems:
Positron In-flight Annihilation (I)

Gamma produced by **annihilation** of a relativistic positron ($\gamma=E_p/m>>1$) on an electron at rest ($E_e=m$):

- (E_γ,θ_γ) correlation: hardening by collimation
- focused forward in cone $\Delta\theta\approx 1/\gamma$: small divergence
- energy range $\Delta E\approx E_{\gamma,max}/2\gamma$: good resolution

$$E_\gamma(\theta_\gamma)=\frac{m}{1-\frac{p_p}{E_p+m}\cos(\theta_\gamma)}$$

E_p=9.5MeV: θ_γ<0.15rad → E_γ=8-10MeV

$$\sigma_\gamma\approx 4\pi r_e^2\frac{\log(1+2\gamma)}{1+2\gamma}$$

where $r_e=2.818\cdot 10^{-13}$cm is the classical electron radius

$\sigma_\gamma\approx$83mb at E_p=9.5MeV

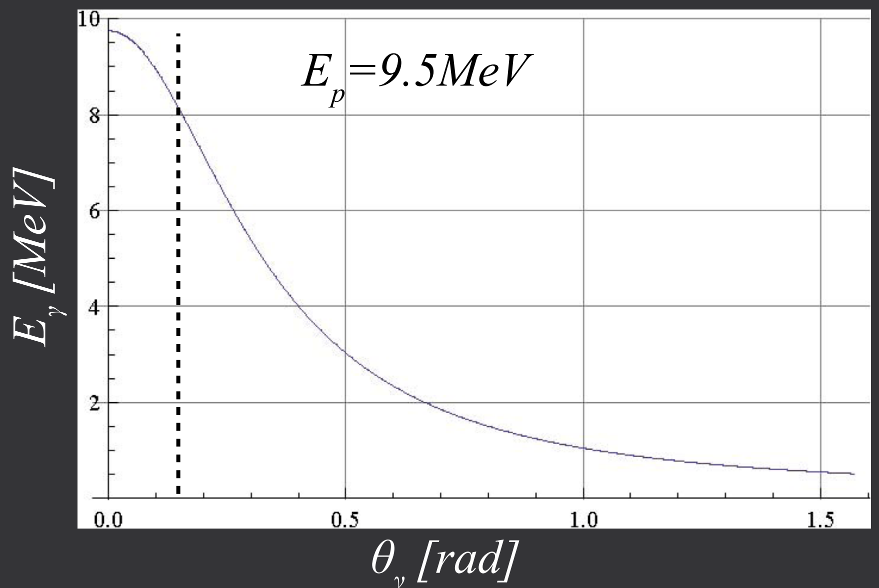

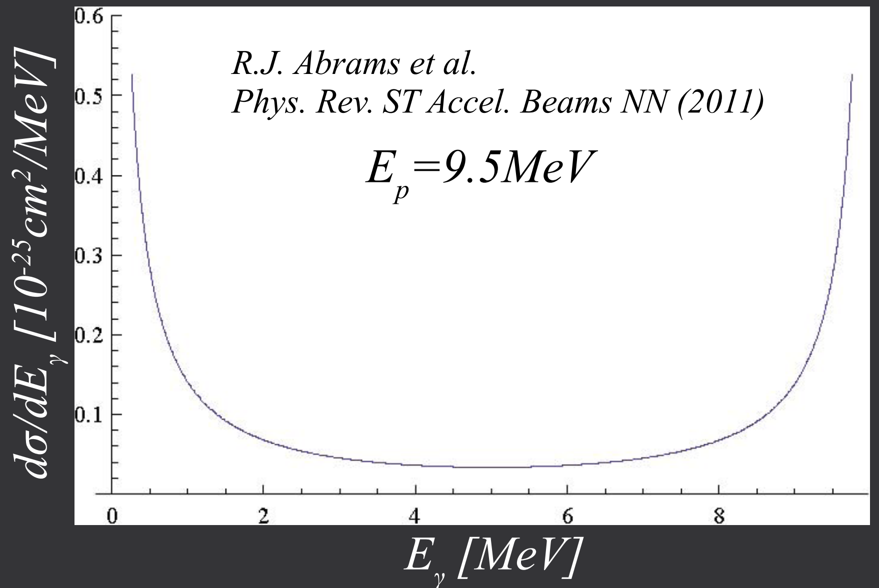

Gamma Beam Systems: Positron In-flight Annihilation (II)

Another improvement of the bremsstrahlung method:

1) convert primary e^- beam to e^+ beam:
   separate e^+ from bremsstrahlung $\gamma \rightarrow e^+e^-$ (target+magnet)
2) prepare secondary e^+ beam:
   reduce energy and angular spread (degrader+magnets)
3) annihilate e^+ beam to final γ beam: radiator

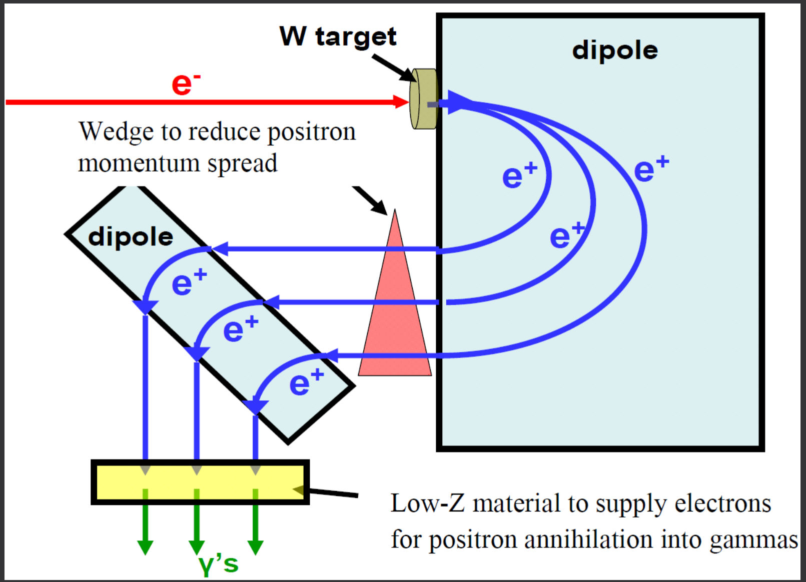

R.J. Abrams et al., Phys. Rev. ST Accel. Beams NN (2011)

Gamma Beam Systems:
Positron In-flight Annihilation (II)

Another improvement of the bremsstrahlung method:

1) convert primary e^- beam to e^+ beam:
   separate e^+ from bremsstrahlung $\gamma \rightarrow e^+e^-$ (target+magnet)
2) prepare secondary e^+ beam:
   reduce energy and angular spread (degrader+magnets)
3) annihilate e^+ beam to final γ beam: radiator

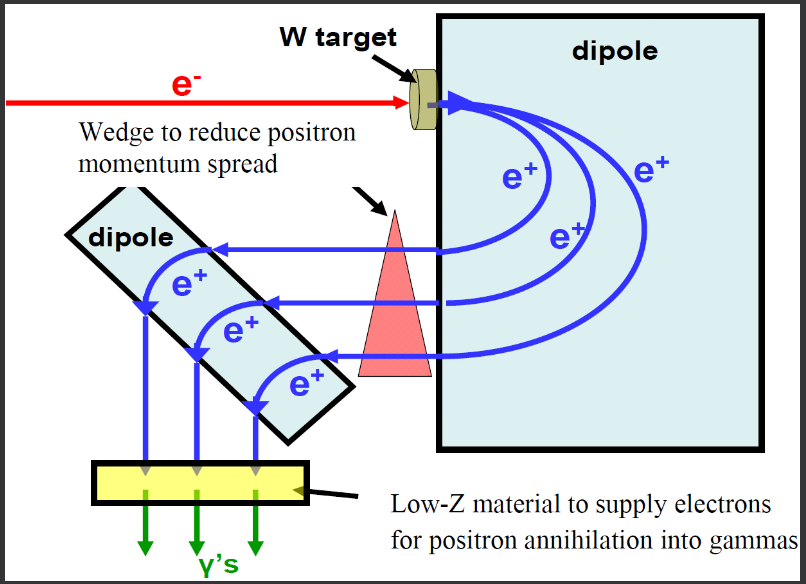

R.J. Abrams et al., Phys. Rev. ST Accel. Beams NN (2011)

- background gammas from bremsstrahlung still present
  $\rightarrow$ deconvolution, lower resolution, shielding
- signal gammas from annihilation form a high-energy peak
  $\rightarrow$ target specific processes
- high intensities are possible:
  10^{15} e^-/s primary beam at 75 MeV $\rightarrow \sim 10^{10}$ γ/s in 8-10MeV

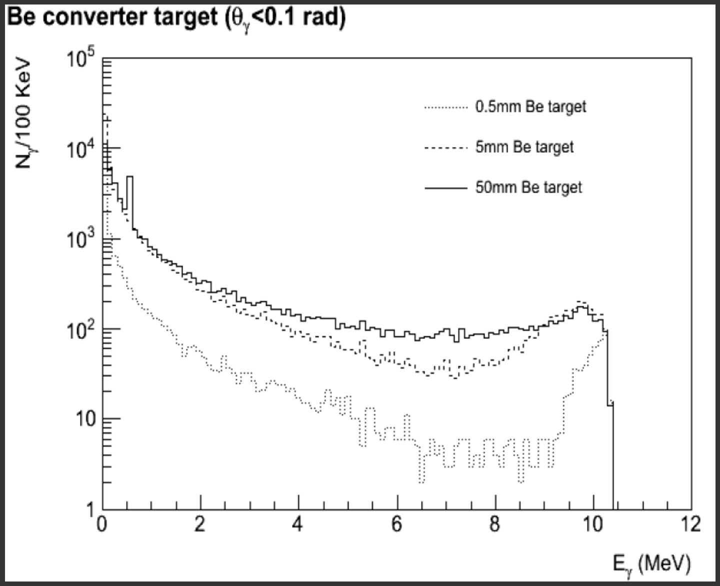

Gamma Beam Systems: Positron In-flight Annihilation (III)

Saclay, France

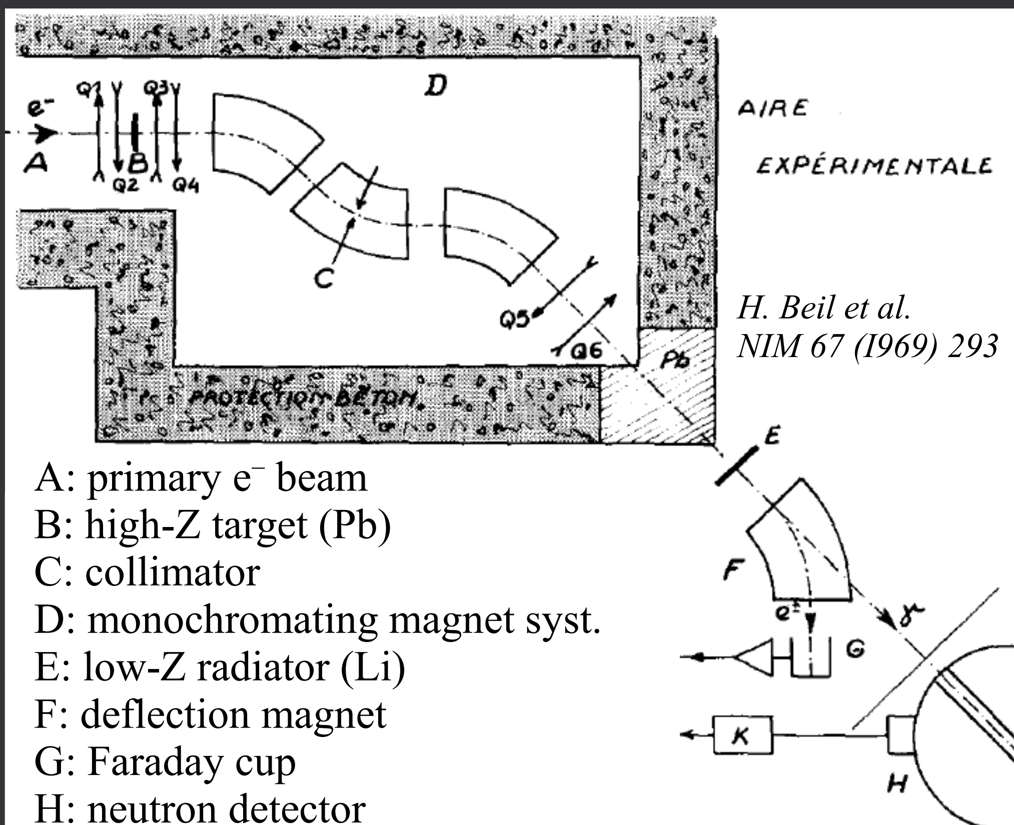

H. Beil et al.
NIM 67 (I969) 293

A: primary e^- beam
B: high-Z target (Pb)
C: collimator
D: monochromating magnet syst.
E: low-Z radiator (Li)
F: deflection magnet
G: Faraday cup
H: neutron detector

Primary electron beam: E = 45MeV
Final gamma beam: E = 5-40MeV
ΔE_γ = 140keV at E_γ = 10MeV

Gamma Beam Systems:
Positron In-flight Annihilation (III)

Saclay, France

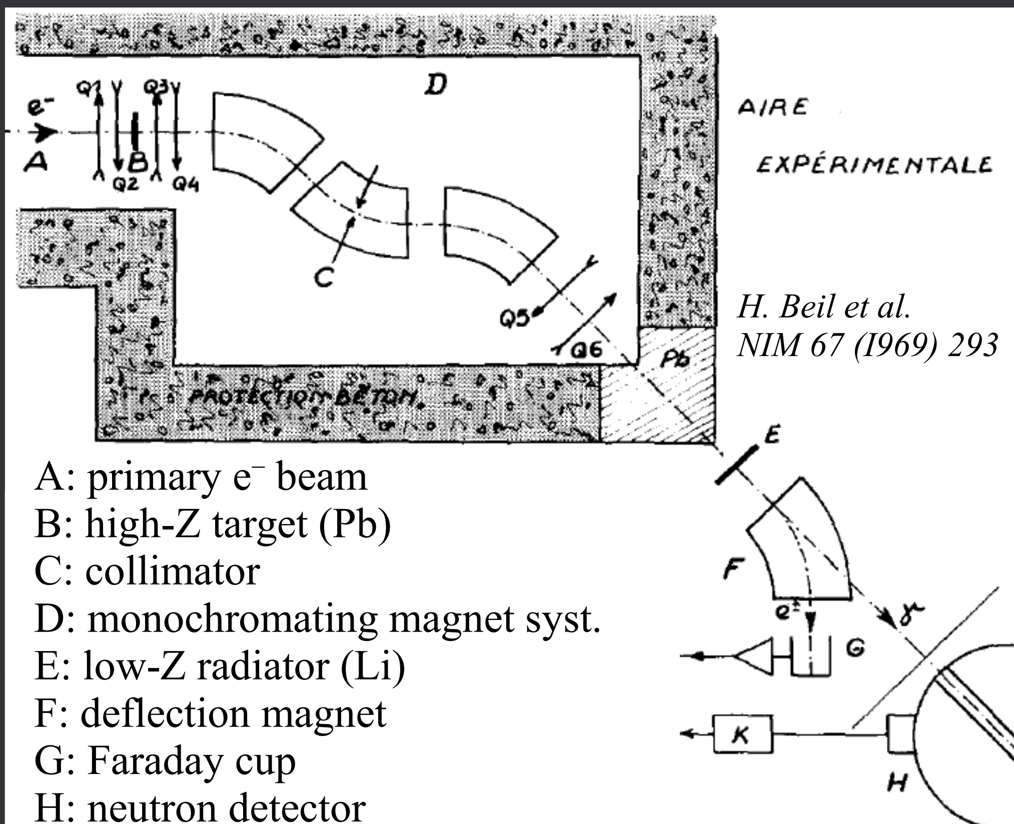

Lawrence Livermore Natl. Lab., USA

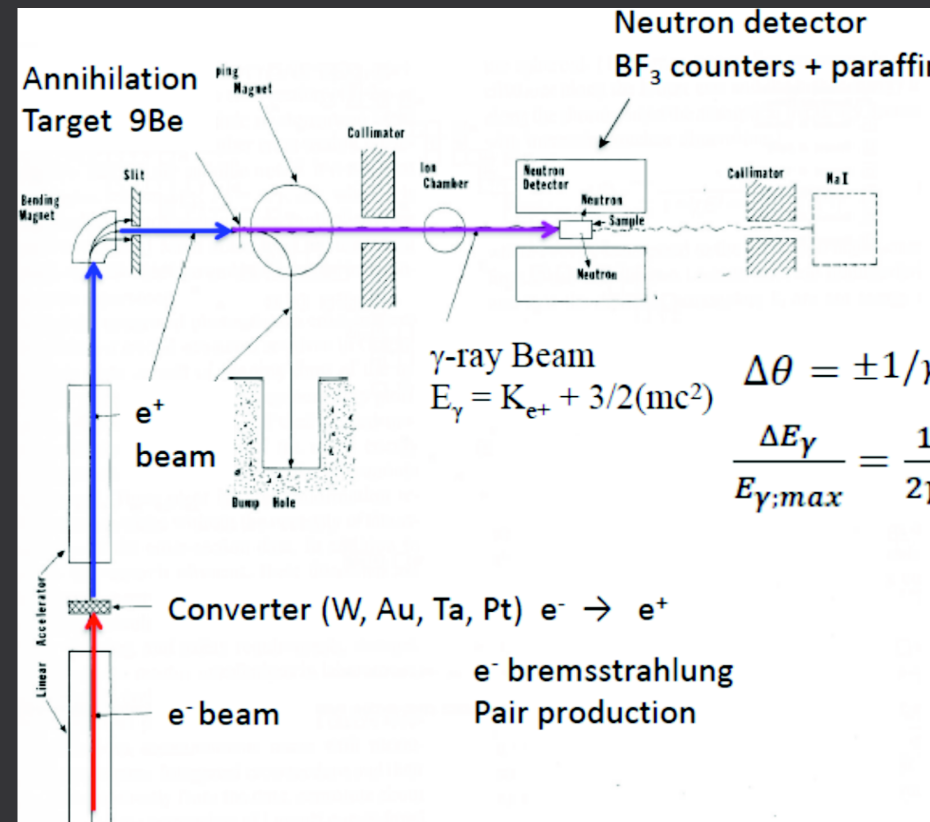

Primary electron beam: E = 45MeV
Final gamma beam: E = 5-40MeV
ΔE_γ = 140keV at E_γ = 10MeV

Gamma Beam Systems: Coulomb Excitation (I)

$E_{beam}<B_C$: standard method to study low-lying collective modes.
Peripheral ($b>R_A+R_B$) ion collisions via virtual photon exchange.

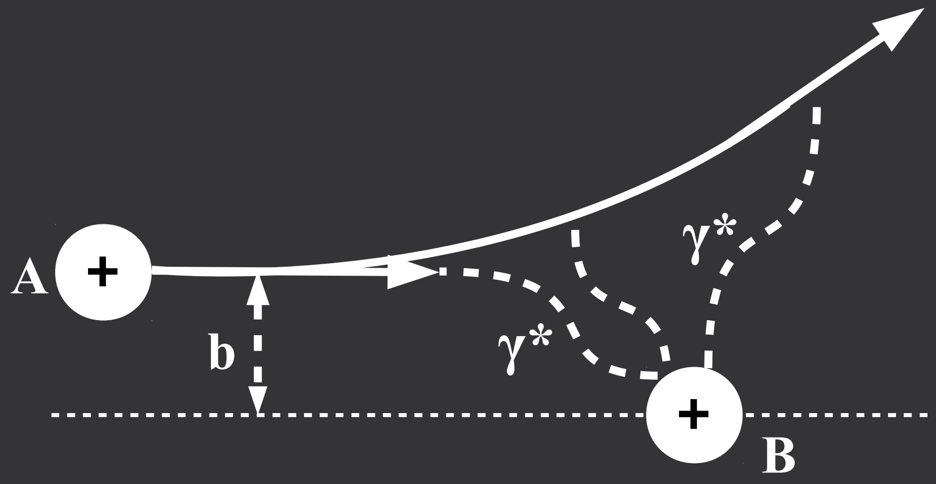

Gamma Beam Systems: Coulomb Excitation (I)

$E_{beam}<B_C$: standard method to study low-lying collective modes.
Peripheral ($b>R_A+R_B$) ion collisions via virtual photon exchange.

– rely on models to get energy distribution
– separate from nuclear reactions: forward $\theta\sim0^o$, various kinematic cuts (e.g. $B\rho/B\rho_0$)

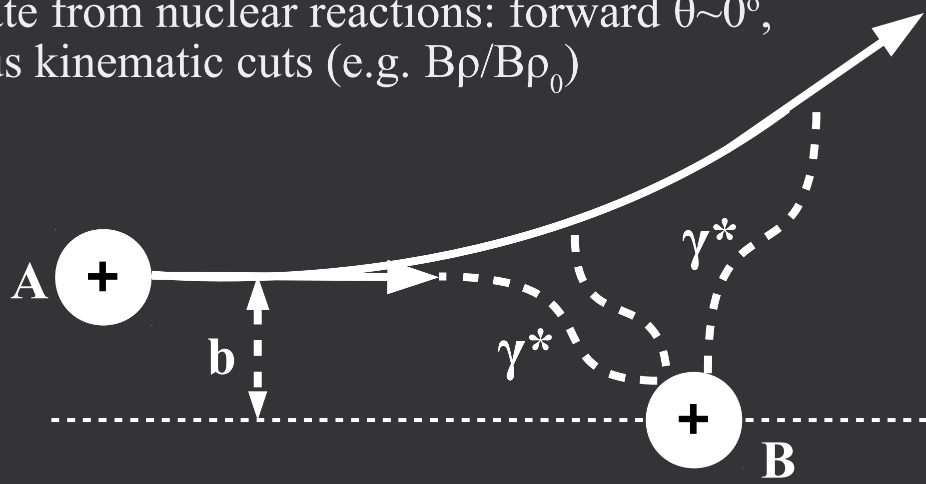

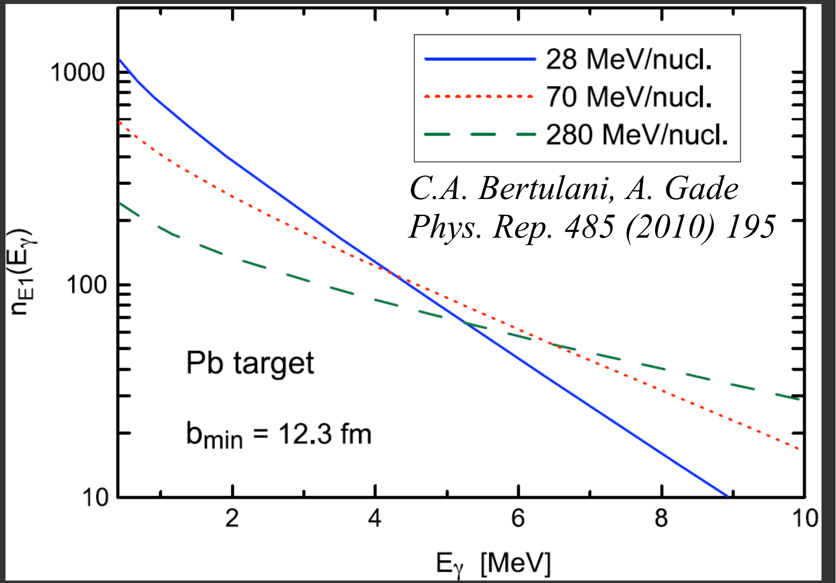

Gamma Beam Systems: Coulomb Excitation (I)

$E_{beam}<B_C$: standard method to study low-lying collective modes.
Peripheral ($b>R_A+R_B$) ion collisions via virtual photon exchange.

– rely on models to get energy distribution
– separate from nuclear reactions: forward θ~0°, various kinematic cuts (e.g. $B\rho/B\rho_0$)

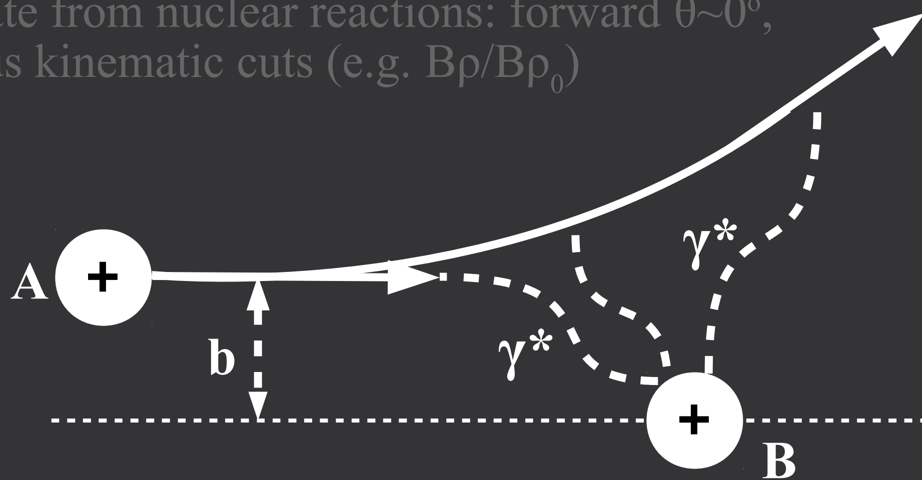

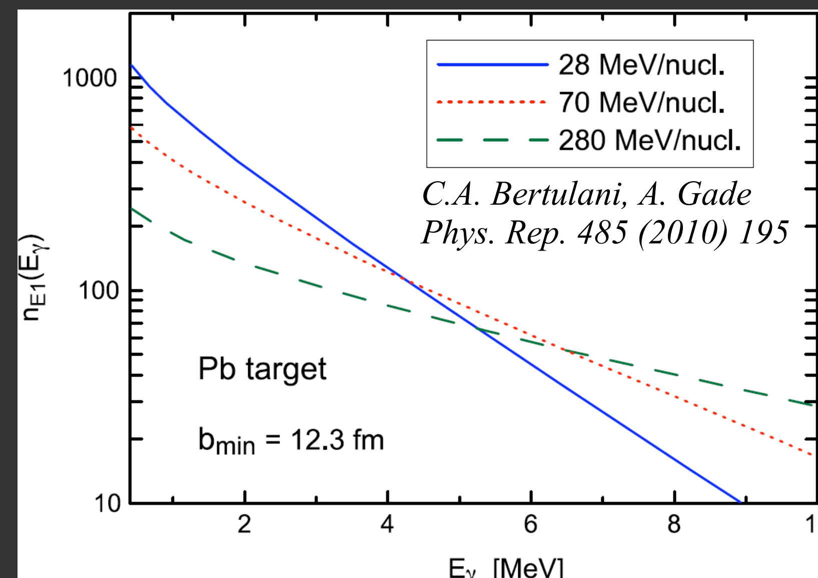

- inelastic (p,p'γ) or (α,α'γ)
  - E1 component is singled out as Coulomb excitation dominant at θ~0°
  - other components (M1) are difficult to separate from nuclear reactions
- inverse kinematics heavy ions
  - used for photo-fission studies (small sensitivity on $\langle E_\gamma^* \rangle$)
  - probablity of electromagnetic reaction increases with Z_A, Z_B and E_{beam}
  - kinematic boost of reaction products: higher energy resolution for both KE and (A,Z)
- radioactive isotope beams
  - replace primary stable beam with secondary radioactive isotope beam

Gamma Beam Systems:
Coulomb Excitation (II)

SOFIA @ GSI:

– ^{238}U beam at 750MeV/n on U and Pb targets → $E_{\gamma*}$<25MeV , σ_{EM}≈2b (σ_{reac}≈13.4b)

Gamma Beam Systems: Coulomb Excitation (II)

SOFIA @ GSI:

– ^{238}U beam at 750MeV/n on U and Pb targets → $E_{\gamma*}$<25MeV , $\sigma_{EM}\approx$2b ($\sigma_{reac}\approx$13.4b)

ΔE-Bρ-TOF measurement:
Active target (ionization chamber): $\Delta E \sim Z^2$
MUSIC(Multiple Sampling Ionization Chambers): $\Delta E \sim Z^2$ (higher resolution)
MWPC (MultiWire Proportional Chamber): (x,y) position for Bρ
ALADIN: large acceptance magnet
Scintillator wall: TOF

E. Pellereau et al., Phys.Rev. C95 (2017) 054603

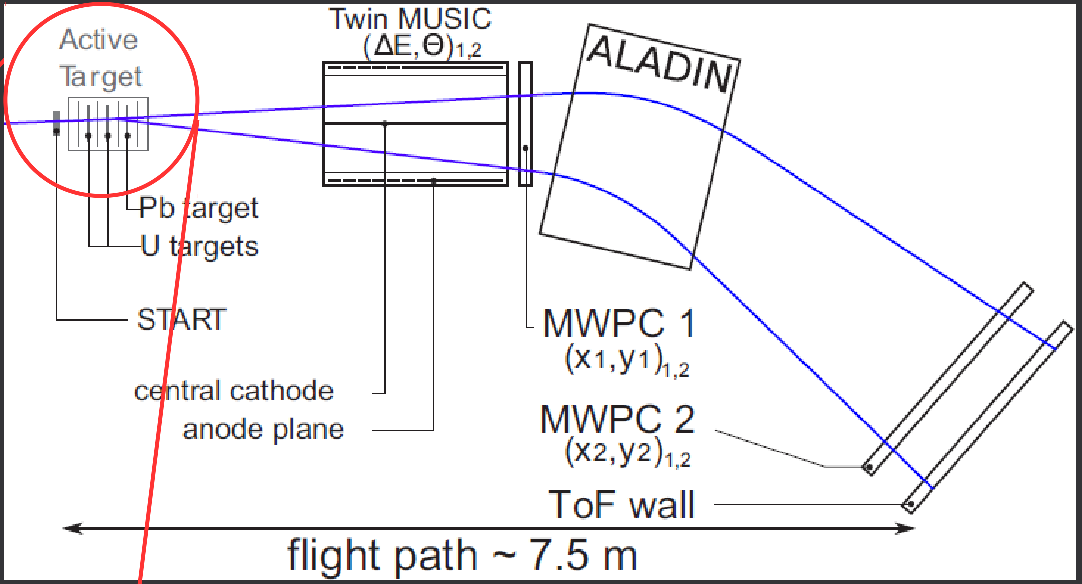

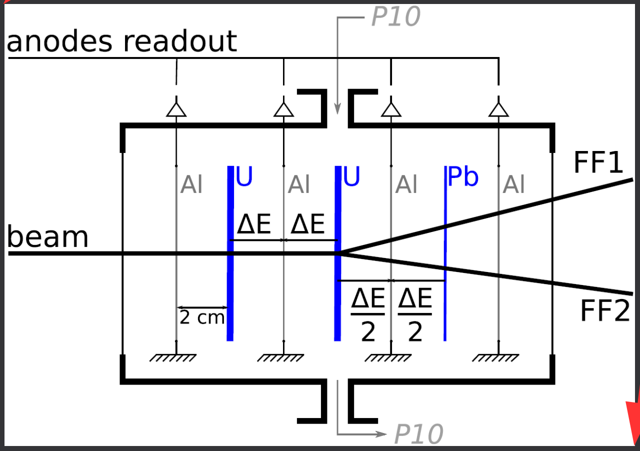

Gamma Beam Systems: Coulomb Excitation (II)

SOFIA @ GSI:

– ^{238}U beam at 750MeV/n on U and Pb targets → $E_{\gamma*}$<25MeV , σ_{EM}≈2b (σ_{reac}≈13.4b)

ΔE-Bρ-TOF measurement:
Active target (ionization chamber): ΔE~Z^2
MUSIC(Multiple Sampling Ionization Chambers): ΔE~Z^2 (higher resolution)
MWPC (MultiWire Proportional Chamber): (x,y) position for Bρ
ALADIN: large acceptance magnet
Scintillator wall: TOF

E. Pellereau et al., Phys.Rev. C95 (2017) 054603

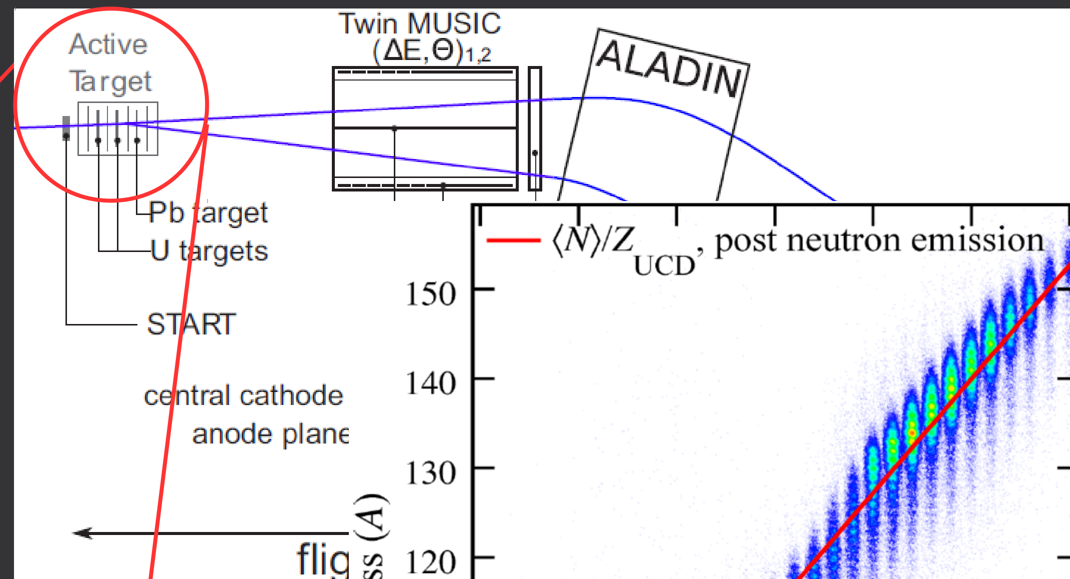

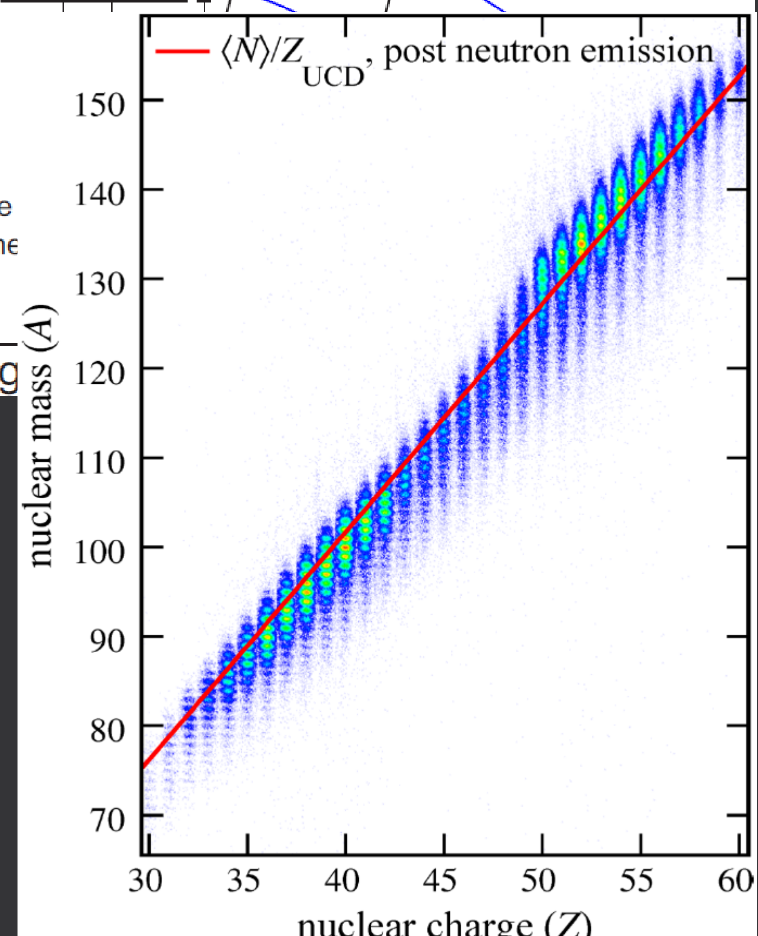

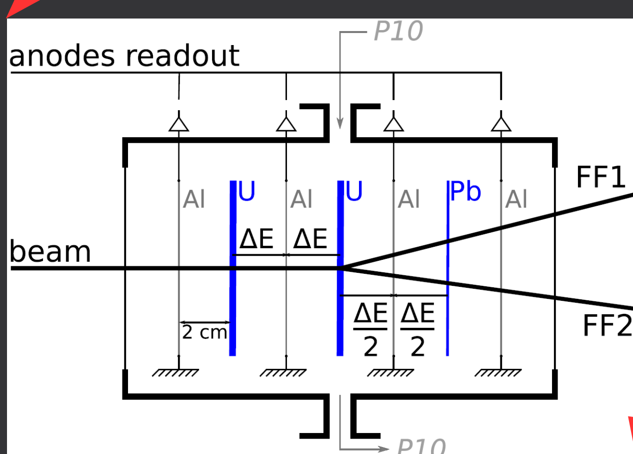

Gamma Beam Systems:
Summary

- Bremsstrahlung:
  - ✔ simplest method to get high γ flux
  - ✗ large ~1/E background: spectrum deconvolution, low ΔE~200keV
  - ✗ small polarization: ranges within 0-40%
  - ✗ no (E,θ) correlation, weak forward focusing

Gamma Beam Systems: Summary

- Bremsstrahlung:
  - ✔ simplest method to get high γ flux
  - ✗ large ~1/E background: spectrum deconvolution, low ΔE~200keV
  - ✗ small polarization: ranges within 0-40%
  - ✗ no (E,θ) correlation, weak forward focusing
- Photon tagging:
  - ✔ significant ΔE improvement (~35keV)
  - ✗ lower γ flux
  - ✗ same problems with large ~1/E background

Gamma Beam Systems: Summary

- Bremsstrahlung:
  - ✔ simplest method to get high γ flux
  - ✗ large ~1/E background: spectrum deconvolution, low ΔE~200keV
  - ✗ small polarization: ranges within 0-40%
  - ✗ no (E,θ) correlation, weak forward focusing
- Photon tagging:
  - ✔ significant ΔE improvement (~35keV)
  - ✗ lower γ flux
  - ✗ same problems with large ~1/E background
- Positron annihilation:
  - ✔ high energy peak: target specific processes, better ΔE than BR
  - ✔ high γ flux
  - ✔ (E,θ) correlation, better forward focusing
  - ✗ large ~1/E background still present

Gamma Beam Systems: Summary

- Bremsstrahlung:
  - ✔ simplest method to get high γ flux
  - ✗ large ~1/E background: spectrum deconvolution, low ΔE~200keV
  - ✗ small polarization: ranges within 0-40%
  - ✗ no (E,θ) correlation, weak forward focusing
- Photon tagging:
  - ✔ significant ΔE improvement (~35keV)
  - ✗ lower γ flux
  - ✗ same problems with large ~1/E background
- Positron annihilation:
  - ✔ high energy peak: target specific processes, better ΔE than BR
  - ✔ high γ flux
  - ✔ (E,θ) correlation, better forward focusing
  - ✗ large ~1/E background still present
- Coulomb excitation:
  - not a γ beam system, its own niche of photonuclear studies

Gamma Beam Systems: Summary

- Bremsstrahlung:
  - ✔ simplest method to get high γ flux
  - ✗ large ~1/E background: spectrum deconvolution, low ΔE~200keV
  - ✗ small polarization: ranges within 0-40%
  - ✗ no (E,θ) correlation, weak forward focusing
- Photon tagging:
  - ✔ significant ΔE improvement (~35keV)
  - ✗ lower γ flux
  - ✗ same problems with large ~1/E background
- Positron annihilation:
  - ✔ high energy peak: target specific processes, better ΔE than BR
  - ✔ high γ flux
  - ✔ (E,θ) correlation, better forward focusing
  - ✗ large ~1/E background still present
- Coulomb excitation:
  - not a γ beam system, its own niche of photonuclear studies

→ Inverse Compton Scattering (ICS) systems are the most promising alternative

Compton Scattering: Kinematics

Photon scattering of an *electron at rest*

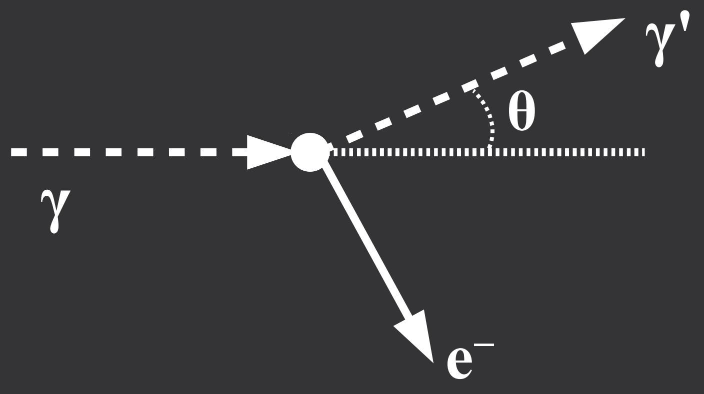

Compton Scattering: Kinematics

Photon scattering of an *electron at rest*

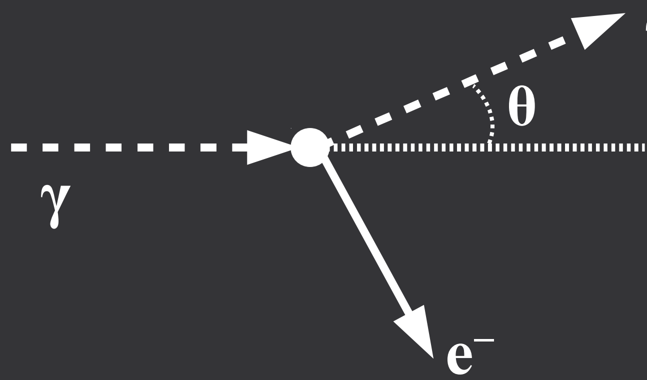

4-momentum conservation: $P_\gamma + P_e = P'_\gamma + P'_e$

photon: $P_\gamma = \frac{\epsilon}{c}(1, \vec{n}), \quad P'_\gamma = \frac{\epsilon'}{c}(1, \vec{n}')$

electron: $P_e = m_e c(1, 0), \quad P'_e = \frac{E}{c}(1, \beta \vec{n}_e)$

$$|P|^2 = P_\mu P^\mu = \eta_{\mu\nu} P^\mu P^\nu = \frac{-E^2}{c^2} + |\vec{p}|^2 = -m^2 c^2$$

Compton Scattering: Kinematics

Photon scattering of an *electron at rest*

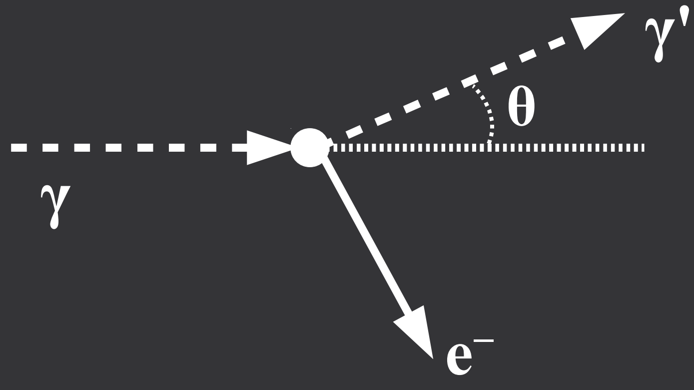

4-momentum conservation: $P_\gamma + P_e = P'_\gamma + P'_e$

photon: $P_\gamma = \frac{\epsilon}{c}(1, \vec{n}), \quad P'_\gamma = \frac{\epsilon'}{c}(1, \vec{n}')$

electron: $P_e = m_e c(1, 0), \quad P'_e = \frac{E}{c}(1, \beta \vec{n}_e)$

$$|P|^2 = P_\mu P^\mu = \eta_{\mu\nu} P^\mu P^\nu = \frac{-E^2}{c^2} + |\vec{p}|^2 = -m^2 c^2$$

$$|P'_e|^2 = |P_\gamma + P_e - P'_\gamma|^2 = |P_\gamma|^2 + |P_e|^2 + |P'_\gamma|^2 + 2 P_\gamma \cdot P_e - 2 P'_\gamma \cdot P_e - 2 P_\gamma \cdot P'_\gamma$$

Compton Scattering: Kinematics

Photon scattering of an *electron at rest*

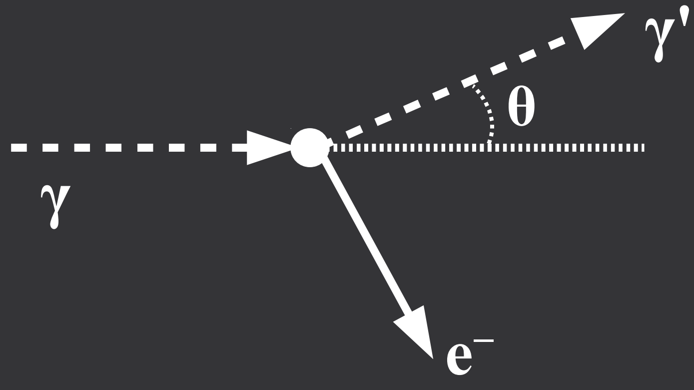

4-momentum conservation: $P_\gamma + P_e = P'_\gamma + P'_e$

photon: $P_\gamma = \frac{\epsilon}{c}(1, \vec{n}), \quad P'_\gamma = \frac{\epsilon'}{c}(1, \vec{n}')$

electron: $P_e = m_e c(1, 0), \quad P'_e = \frac{E}{c}(1, \beta \vec{n}_e)$

$$|P|^2 = P_\mu P^\mu = \eta_{\mu\nu} P^\mu P^\nu = \frac{-E^2}{c^2} + |\vec{p}|^2 = -m^2 c^2$$

$$|P'_e|^2 = |P_\gamma + P_e - P'_\gamma|^2 = |P_\gamma|^2 + |P_e|^2 + |P'_\gamma|^2 + 2 P_\gamma \cdot P_e - 2 P'_\gamma \cdot P_e - 2 P_\gamma \cdot P'_\gamma$$

$$-m_e^2 c^2 = 0 - m_e^2 c^2 + 0 + 2\left(-\frac{\epsilon}{c} m_e c\right) - 2\left(-\frac{\epsilon'}{c} m_e c\right) - 2\left(-\frac{\epsilon\epsilon'}{c^2} + \frac{\epsilon\epsilon'}{c^2} \vec{n} \cdot \vec{n}'\right)$$

$$\epsilon m_e - \epsilon' m_e - \frac{\epsilon\epsilon'}{c^2}(1 - \vec{n} \cdot \vec{n}') = 0 \;\Rightarrow\; \epsilon m_{ec}^2 = \epsilon' m_{ec}^2 + \epsilon\epsilon'(1 - \cos(\theta)) \;\Rightarrow\; \boxed{\epsilon' = \frac{\epsilon}{1 + \frac{\epsilon}{m_e c^2}(1 - \cos(\theta))}}$$

Compton Scattering: Kinematics

Photon scattering of an *electron at rest*

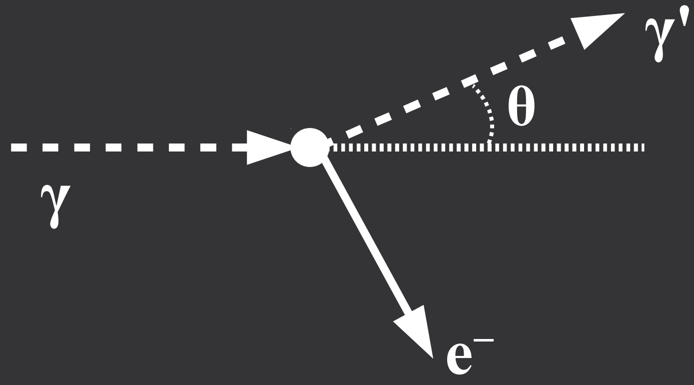

4-momentum conservation: $P_\gamma + P_e = P'_\gamma + P'_e$

photon: $P_\gamma = \frac{\epsilon}{c}(1, \vec{n}), \quad P'_\gamma = \frac{\epsilon'}{c}(1, \vec{n}')$

electron: $P_e = m_e c(1, 0), \quad P'_e = \frac{E}{c}(1, \beta \vec{n}_e)$

$$|P|^2 = P_\mu P^\mu = \eta_{\mu\nu} P^\mu P^\nu = \frac{-E^2}{c^2} + |\vec{p}|^2 = -m^2 c^2$$

$$|P'_e|^2 = |P_\gamma + P_e - P'_\gamma|^2 = |P_\gamma|^2 + |P_e|^2 + |P'_\gamma|^2 + 2P_\gamma \cdot P_e - 2P'_\gamma \cdot P_e - 2P_\gamma \cdot P'_\gamma$$

$$-m_e^2 c^2 = 0 - m_e^2 c^2 + 0 + 2\left(-\frac{\epsilon}{c} m_e c\right) - 2\left(-\frac{\epsilon'}{c} m_e c\right) - 2\left(-\frac{\epsilon\epsilon'}{c^2} + \frac{\epsilon\epsilon'}{c^2} \vec{n} \cdot \vec{n}'\right)$$

$$\epsilon m_e - \epsilon' m_e - \frac{\epsilon\epsilon'}{c^2}(1 - \vec{n} \cdot \vec{n}') = 0 \;\Rightarrow\; \epsilon m_{ec}^2 = \epsilon' m_{ec}^2 + \epsilon\epsilon'(1 - \cos(\theta)) \;\Rightarrow$$

$$\boxed{\epsilon' = \frac{\epsilon}{1 + \frac{\epsilon}{m_e c^2}(1 - \cos(\theta))}}$$

Thomson scattering (up to soft X-rays): $\varepsilon \ll m_e c^2 = 511\,\text{keV} \rightarrow \varepsilon' \approx \varepsilon$

Compton Scattering: Cross Section (I)

Fyenman diagrams at tree level:

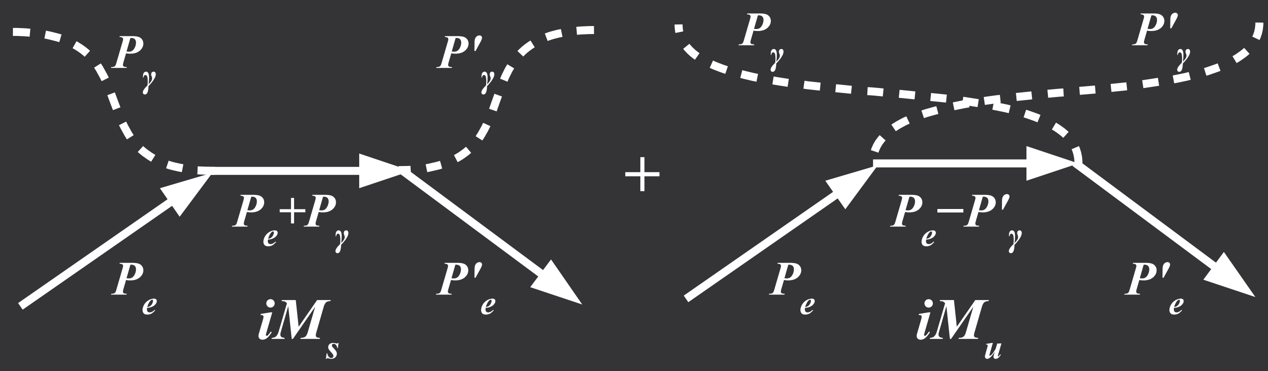

Compton Scattering: Cross Section (I)

Fyenman diagrams at tree level:

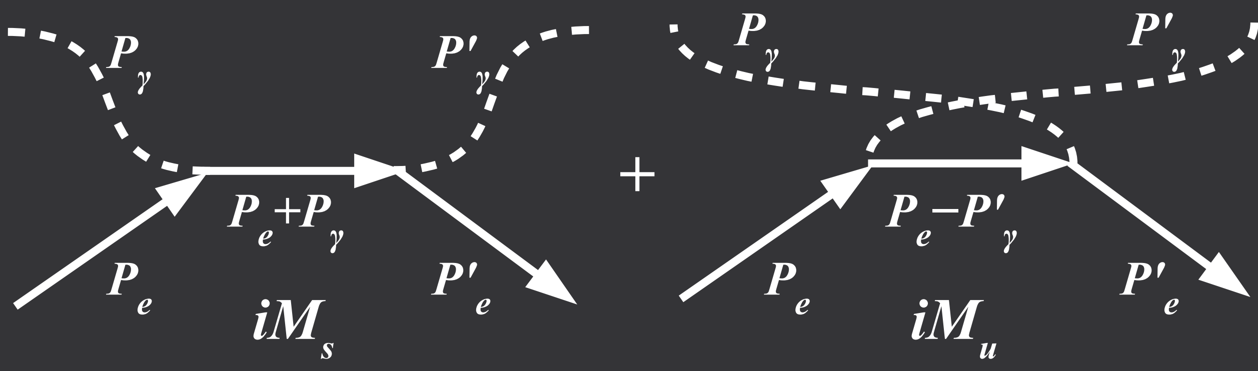

Mandelstam variables:

$s = (P_e+P_\gamma)^2 = m^2+2\underline{p}_e\cdot\underline{p}_\gamma$

$u = (P_e-P'_\gamma)^2 = m^2-2\underline{p}_e\cdot\underline{p}'_\gamma$

$t = (P'_\gamma-P_\gamma)^2 = -2\underline{p}'_\gamma\cdot\underline{p}_\gamma$

$s + u + t = 2m^2$

Dimensionless variables:

$x \equiv +(s-m^2)/m^2 = 2\underline{p}_e\cdot\underline{p}_\gamma/m^2$

$y \equiv -(u-m^2)/m^2 = 2\underline{p}_e\cdot\underline{p}'_\gamma/m^2$

$z \equiv -t/m^2 \qquad = 2\underline{p}'_\gamma\cdot\underline{p}_\gamma/m^2$

Compton Scattering: Cross Section (I)

Fyenman diagrams at tree level:

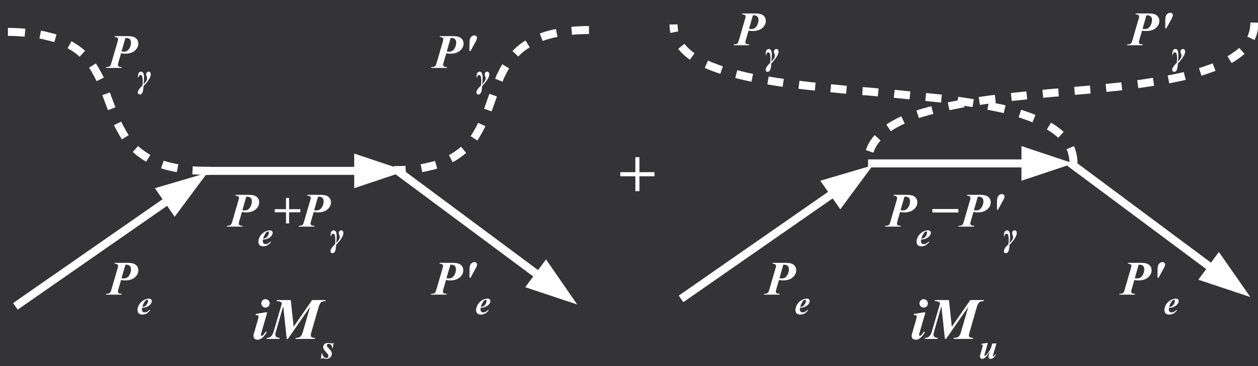

Mandelstam variables:

$s = (P_e+P_\gamma)^2 = m^2+2p_e \cdot p_\gamma$

$u = (P_e-P'_\gamma)^2 = m^2-2p_e \cdot p'_\gamma$

$t = (P'_\gamma-P_\gamma)^2 = -2p'_\gamma \cdot p_\gamma$

$s + u + t = 2m^2$

Dimensionless variables:

$x \equiv +(s-m^2)/m^2 = 2p_e \cdot p_\gamma/m^2$

$y \equiv -(u-m^2)/m^2 = 2p_e \cdot p'_\gamma/m^2$

$z \equiv -t/m^2 \qquad = 2p'_\gamma \cdot p_\gamma/m^2$

Scattering probability (integrated over spins ξ,ξ' and polarizations λ,λ'):

$$|M|^2 = \frac{1}{4}\sum_{\xi,\xi'=1}^{2}\sum_{\lambda,\lambda'}|M_s+M_u|^2 = 8e^4\left[\left(\frac{1}{x}-\frac{1}{y}\right)^2+\left(\frac{1}{x}-\frac{1}{y}\right)+\frac{1}{4}\left(\frac{x}{y}+\frac{y}{x}\right)\right]$$

Compton Scattering: Cross Section (I)

Fyenman diagrams at tree level:

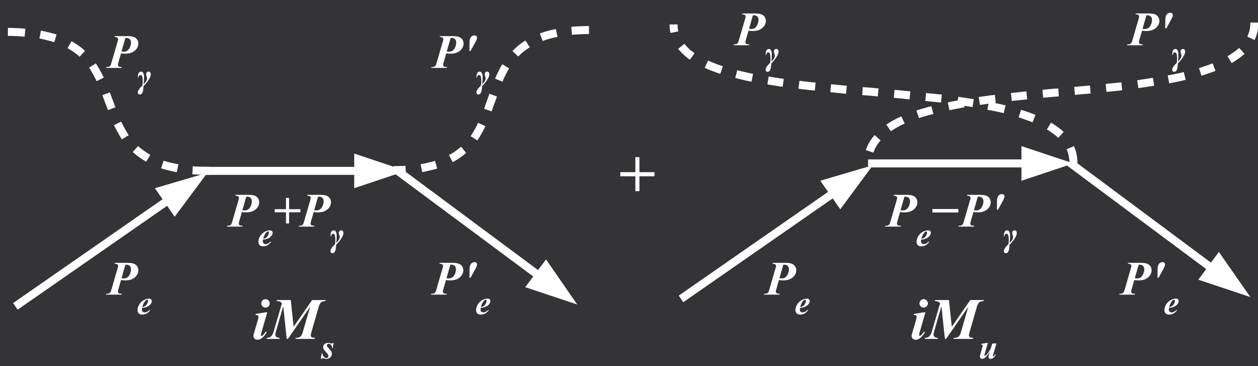

Mandelstam variables:

$s = (P_e+P_\gamma)^2 = m^2+2\bar{p}_e\cdot\bar{p}_\gamma$

$u = (P_e-P'_\gamma)^2 = m^2-2\bar{p}_e\cdot\bar{p}'_\gamma$

$t = (P'_\gamma-P_\gamma)^2 = -2\bar{p}'_\gamma\cdot\bar{p}_\gamma$

$s + u + t = 2m^2$

Dimensionless variables:

$x \equiv +(s-m^2)/m^2 = 2\bar{p}_e\cdot\bar{p}_\gamma/m^2$

$y \equiv -(u-m^2)/m^2 = 2\bar{p}_e\cdot\bar{p}'_\gamma/m^2$

$z \equiv -t/m^2 \qquad = 2\bar{p}'_\gamma\cdot\bar{p}_\gamma/m^2$

Scattering probability (integrated over spins ξ,ξ' and polarizations λ,λ'):

$$|M|^2=\frac{1}{4}\sum_{\xi,\xi'=1}^{2}\sum_{\lambda,\lambda'}|M_s+M_u|^2=8e^4\left[\left(\frac{1}{x}-\frac{1}{y}\right)^2+\left(\frac{1}{x}-\frac{1}{y}\right)+\frac{1}{4}\left(\frac{x}{y}+\frac{y}{x}\right)\right]$$

$$d\sigma=\frac{(2\pi)^4}{4p_e p_\gamma}\cdot|M|^2\cdot\underbrace{\delta^4(P_e+P_\gamma-P'_e-P'_\gamma)\frac{d^3p'_e}{(2\pi)^3 2E'_e}\frac{d^3p'_\gamma}{(2\pi)^3 2E'_\gamma}}_{\text{final state phase space factor}}=\frac{\pi r_e^2}{e^4}|M|^2\frac{dy}{x^2}$$

classical electron radius: $r_e\equiv\frac{\hbar\alpha}{m_e c}\approx 2.82\,fm$

For full calculation: L.D. Landau and E.M. Lifshitz “Quantum Electrodynamics”

Compton Scattering: Cross Section (II)

In the laboratory frame (with θ and θ' the initial and final photon angles w.r.t. electron):

$$x=2\frac{E_e\epsilon}{m^2c^4}(1-\beta\cos(\theta));\quad y=2\frac{E_e\epsilon'}{m^2c^4}(1-\beta\cos(\theta')) \Rightarrow \frac{d\sigma_{KN}}{d\Omega'}=\frac{1}{2}r_e^2\frac{\epsilon'^2}{\epsilon^2}\left(\frac{\epsilon}{\epsilon'}+\frac{\epsilon'}{\epsilon}-\sin^2(\theta')\right)$$

Klein-Nishina equation

at high energies Compton scattering is forward peaked

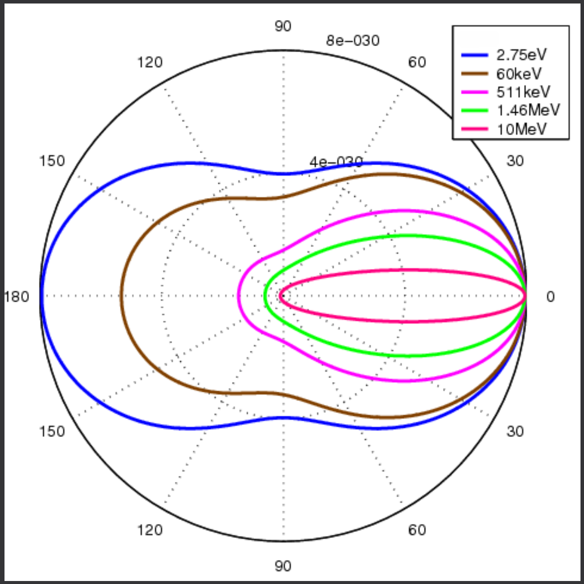

Compton Scattering: Cross Section (II)

In the laboratory frame (with θ and θ' the initial and final photon angles w.r.t. electron):

$$x = 2\frac{E_e \epsilon}{m^2 c^4}(1-\beta\cos(\theta));\quad y = 2\frac{E_e \epsilon'}{m^2 c^4}(1-\beta\cos(\theta')) \Rightarrow \frac{d\sigma_{KN}}{d\Omega'} = \frac{1}{2} r_e^2 \frac{\epsilon'^2}{\epsilon^2}\left(\frac{\epsilon}{\epsilon'} + \frac{\epsilon'}{\epsilon} - \sin^2(\theta')\right)$$

Klein-Nishina equation

Thomson scattering (up to soft X-rays): $\varepsilon \ll m_e c^2 = 511\mathrm{keV} \rightarrow \varepsilon' \approx \varepsilon$

$$\frac{d\sigma_T}{d\Omega'} = \frac{1}{2} r_e^2 (1-\cos^2(\theta'))$$

at high energies Compton scattering is forward peaked

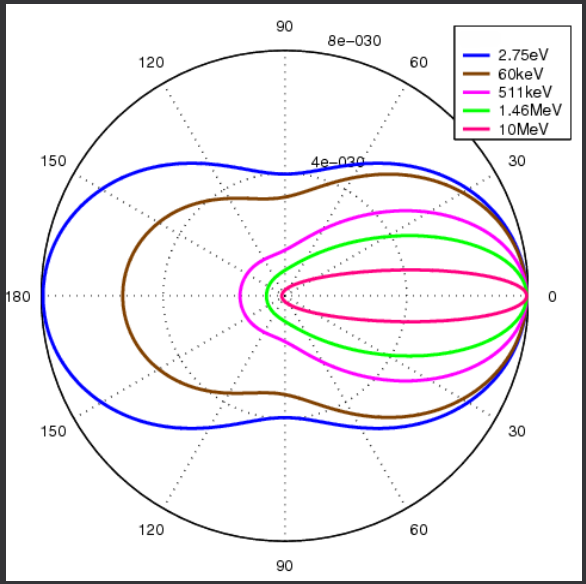

Compton Scattering: Cross Section (II)

In the laboratory frame (with θ and θ' the initial and final photon angles w.r.t. electron):

$$x=2\frac{E_e\epsilon}{m^2c^4}(1-\beta\cos(\theta));\quad y=2\frac{E_e\epsilon'}{m^2c^4}(1-\beta\cos(\theta')) \Rightarrow \frac{d\sigma_{KN}}{d\Omega'}=\frac{1}{2}r_e^2\frac{\epsilon'^2}{\epsilon^2}\left(\frac{\epsilon}{\epsilon'}+\frac{\epsilon'}{\epsilon}-\sin^2(\theta')\right)$$

Klein-Nishina equation

Thomson scattering (up to soft X-rays): $\varepsilon \ll m_e c^2 = 511\,\text{keV} \rightarrow \varepsilon' \approx \varepsilon$

$$\frac{d\sigma_T}{d\Omega'}=\frac{1}{2}r_e^2(1-\cos^2(\theta'))$$

at high energies Compton scattering is forward peaked

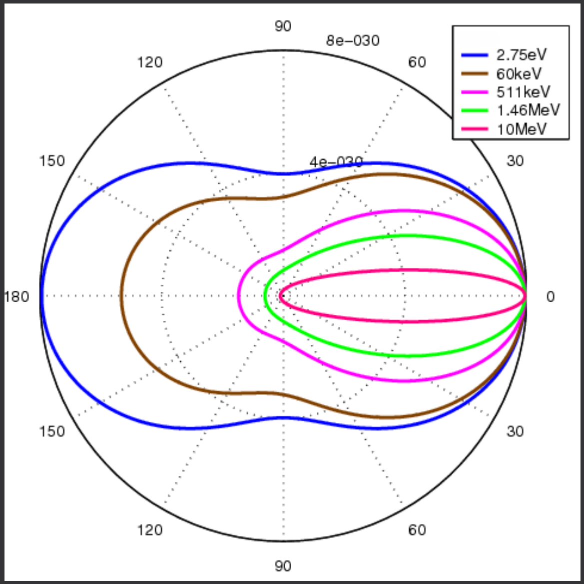

Final photon Stokes vector $\bar{\xi}'=(\xi'_x,\xi'_y,\xi'_z)$ has a more complicated dependence on the initial photon Stokes vector $\bar{\xi}=(\xi_x,\xi_y,\xi_z)$, but **at high energies polarization is almost entirely transferred**!

Compton Scattering: Inverse Kinematics

Inverse Compton Scattering (ICS): Compton scattering of a low energy laser photon (~eV) on an ultra-relativistic electron (hundreds MeV).

Compton Scattering: Inverse Kinematics

Inverse Compton Scattering (ICS): Compton scattering of a low energy laser photon (~eV) on an ultra-relativistic electron (hundreds MeV).

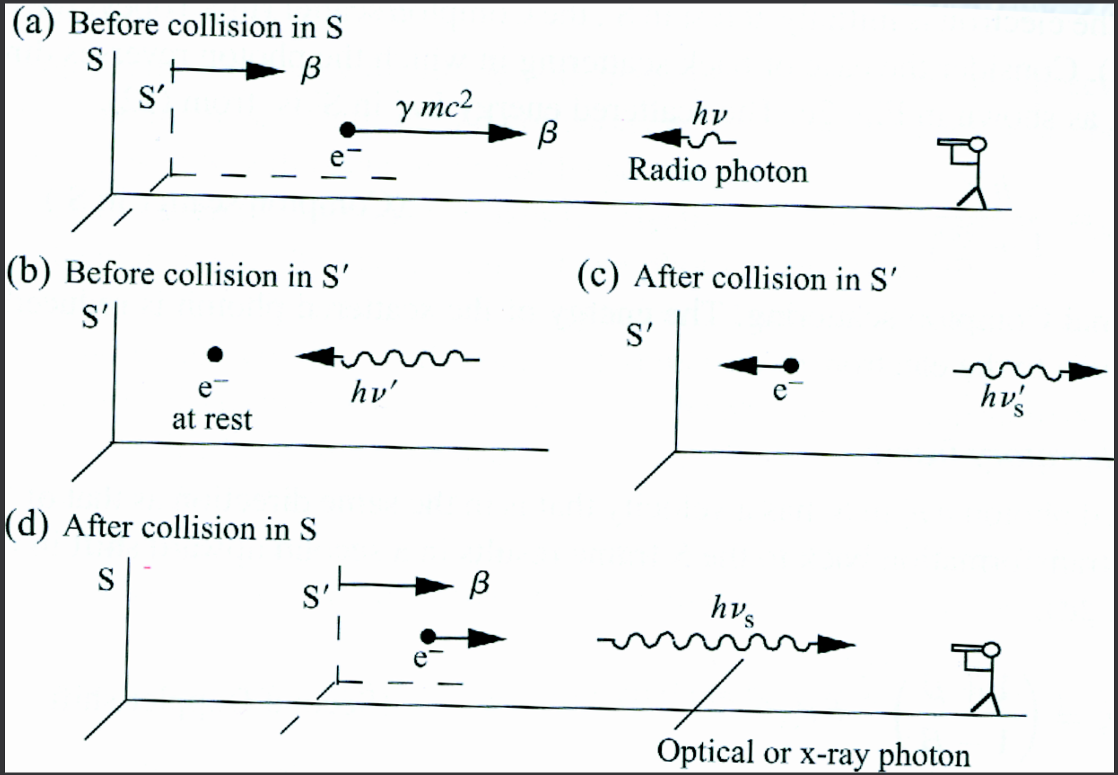

S: laboratory frame

S': electron rest frame

γ>>1: electron's relativistic factor

Compton Scattering: Inverse Kinematics

Inverse Compton Scattering (ICS): Compton scattering of a low energy laser photon (~eV) on an ultra-relativistic electron (hundreds MeV).

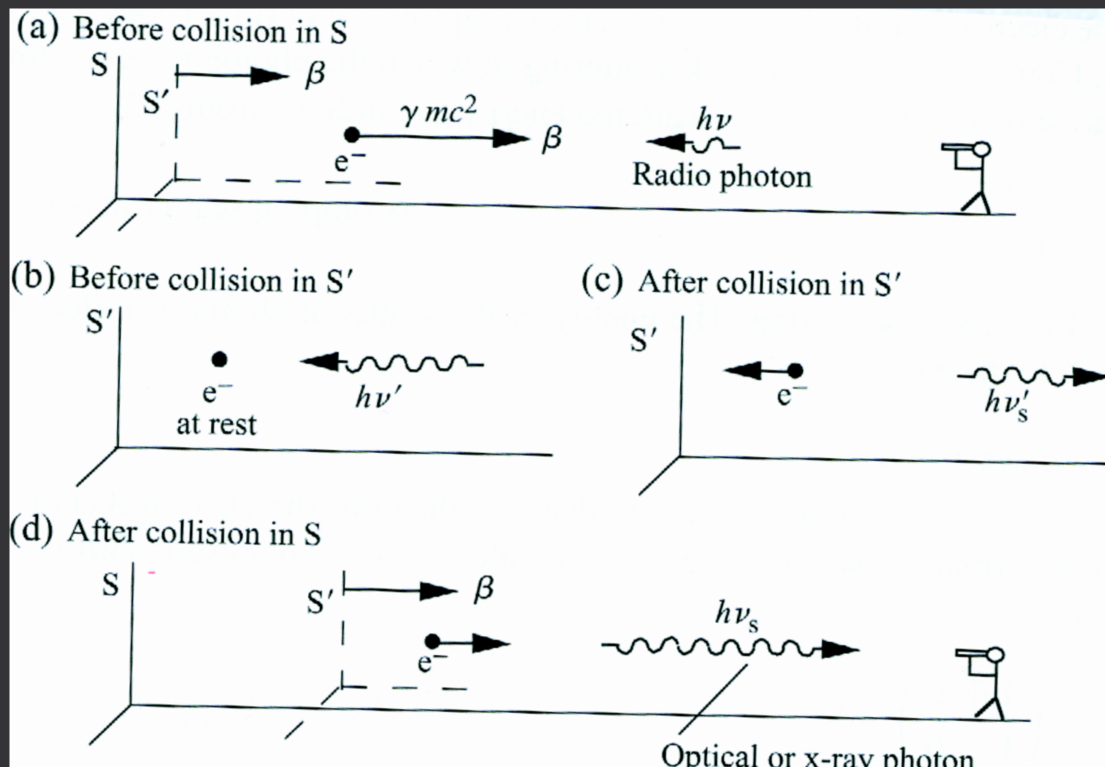

S: laboratory frame

S': electron rest frame

$\gamma >> 1$: electron's relativistic factor

(a) frame S before collision: high-energy electron and low-energy photon move towards each other
(b) frame S' before collision: Lorentz boost of the photon to S' $\rightarrow h\nu' \approx \gamma(1+\beta)h\nu$
(c) frame S' after collision: energy correction due to small electron recoil $\Delta \rightarrow h\nu'_s \approx h\nu' - \Delta$
(d) frame S after collision: Lorentz boost of the photon to S $\rightarrow h\nu_s \approx \gamma(1+\beta)h\nu'_s$

Compton Scattering: Inverse Kinematics

Inverse Compton Scattering (ICS): Compton scattering of a low energy laser photon (~eV) on an ultra-relativistic electron (hundreds MeV).

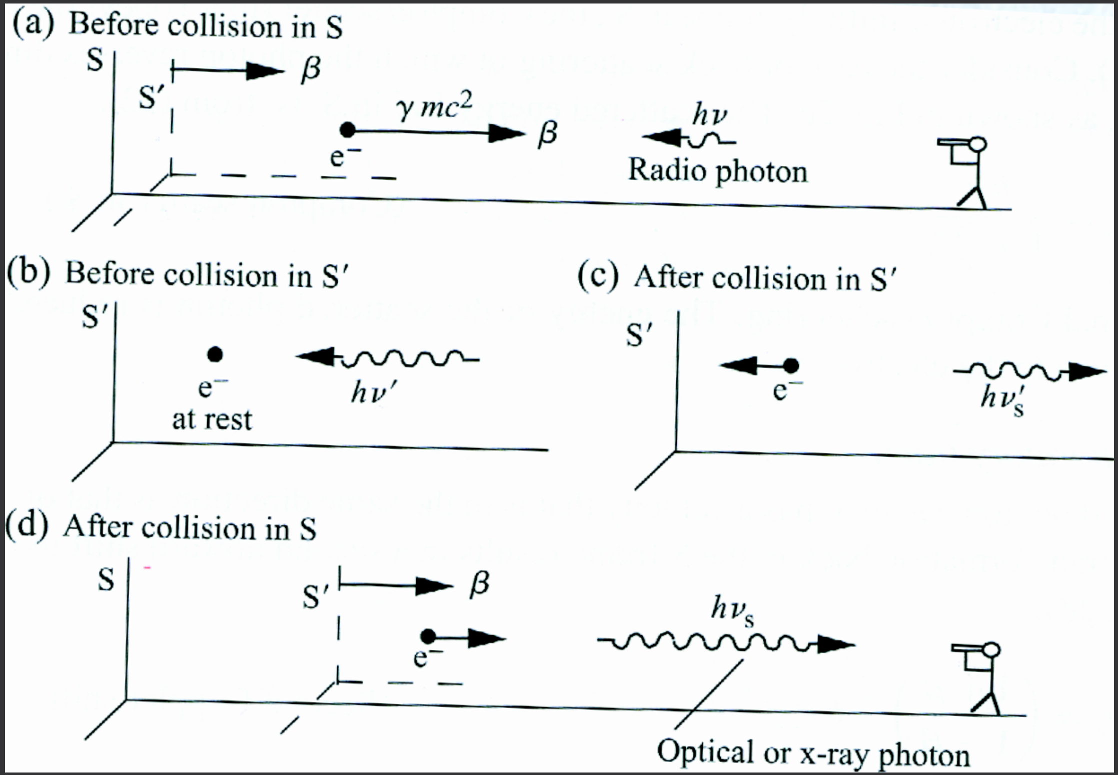

S: laboratory frame

S': electron rest frame

γ>>1: electron's relativistic factor

(a) frame S before collision: high-energy electron and low-energy photon move towards each other
(b) frame S' before collision: Lorentz boost of the photon to S' → $h\nu' \approx \gamma(1+\beta)h\nu$
(c) frame S' after collision: energy correction due to small electron recoil Δ → $h\nu'_s \approx h\nu' - \Delta$
(d) frame S after collision: Lorentz boost of the photon to S → $h\nu_s \approx \gamma(1+\beta)h\nu'_s$

$$\epsilon' \approx \gamma^2(1+\beta)^2\epsilon \approx 4\gamma^2\epsilon$$

Example: ε=2.4eV, E_e=720MeV, γ=1410 → $\varepsilon' \approx$19MeV

Inverse Compton Scattering at ELI-NP

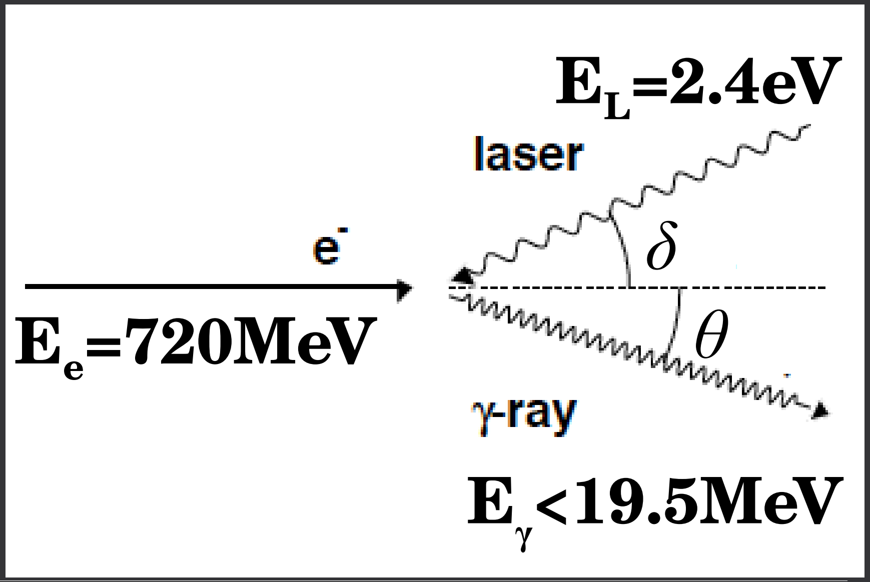

Inverse Compton Scattering at ELI-NP

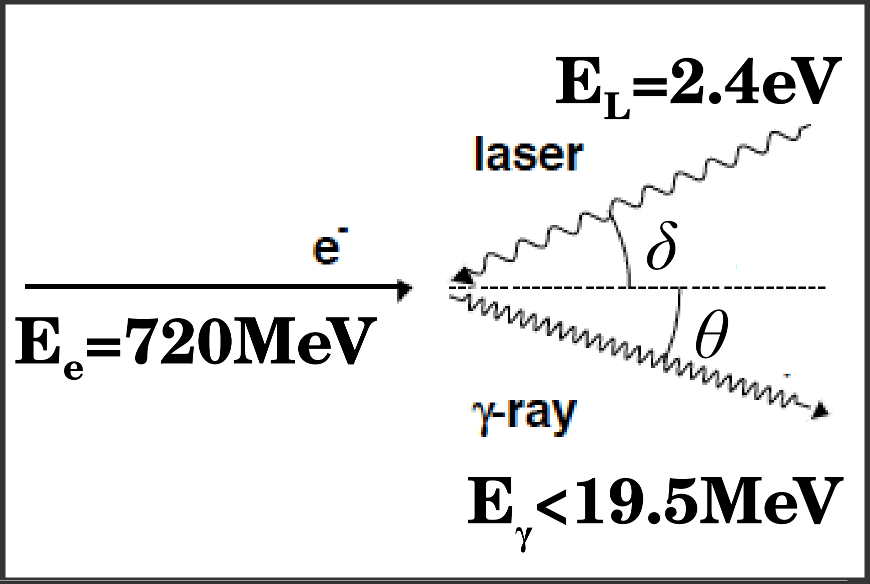

O. Adriani et al., arXiv:1407.3669 (2014)

$$E_\gamma = 2\gamma_e^2 E_L \frac{1+\cos\delta}{1+\frac{a_0^2}{2}+\frac{\delta^2}{4}+(\gamma_e\theta)^2}(1-\Delta)$$

Δ = electron recoil term < 3%

$$a_0 \equiv 2.15\frac{\lambda_L}{w_0}\sqrt{\frac{U}{\sigma_t}}$$

= laser parameter (dimensionless amplitude of the vector potential associated to the laser e.m. field)

Inverse Compton Scattering at ELI-NP

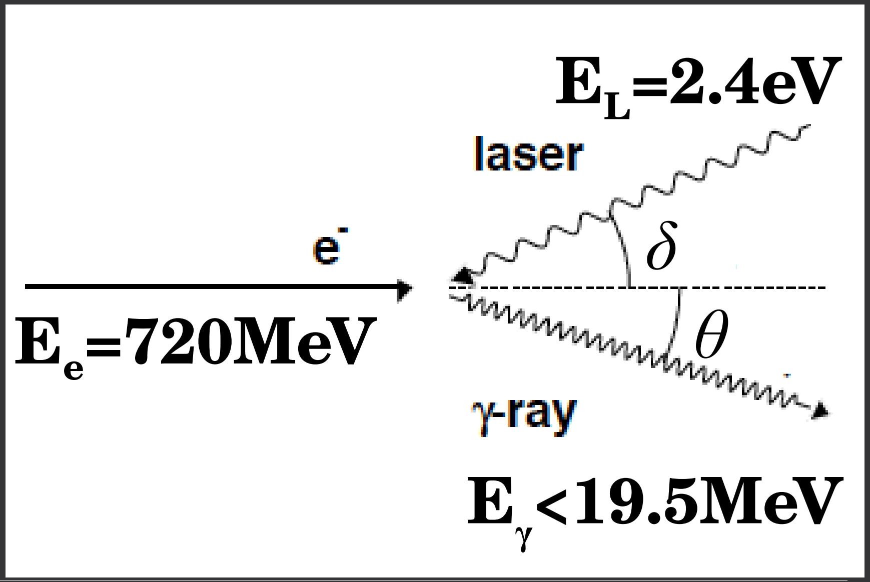

O. Adriani et al., arXiv:1407.3669 (2014)

$$E_\gamma = 2\gamma_e^2 E_L \frac{1+\cos\delta}{1+\frac{a_0^2}{2}+\frac{\delta^2}{4}+(\gamma_e\theta)^2}(1-\Delta)$$

Δ = electron recoil term < 3%

$$a_0 \equiv 2.15\frac{\lambda_L}{w_0}\sqrt{\frac{U}{\sigma_t}}$$

= laser parameter (dimensionless amplitude of the vector potential associated to the laser e.m. field)

Typical laser parameters:
– angle $\delta\approx 7^o \rightarrow 1+\cos\delta\approx 2+10^{-6}$, $\delta^2/4\approx 0.004$
– wavelength λ_L=0.5µm, focal spot w_0=25µm, pulse energy U=0.5J, pulse time σ_t=1.5ps $\rightarrow a_0^2\approx 2.5\cdot 10^{-3}$

Inverse Compton Scattering at ELI-NP

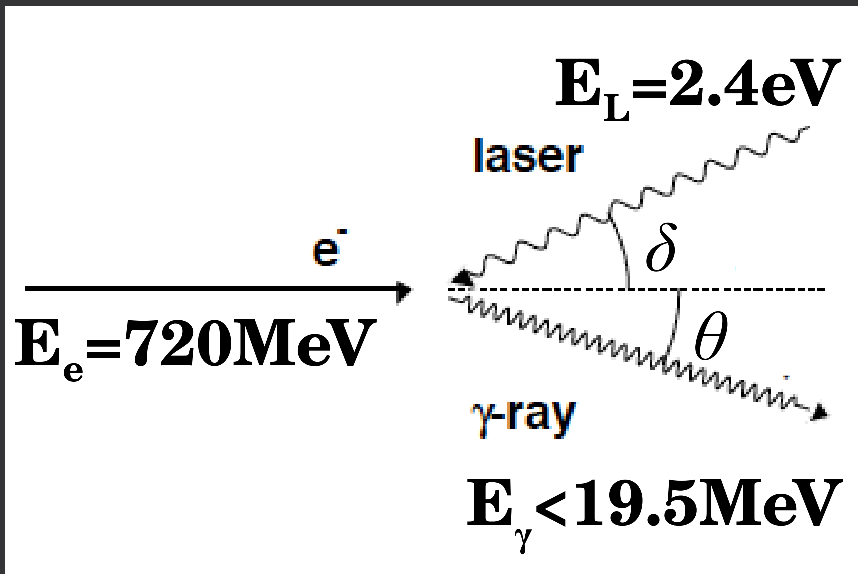

O. Adriani et al., arXiv:1407.3669 (2014)

$$E_\gamma = 2\gamma_e^2 E_L \frac{1+\cos\delta}{1+\frac{a_0^2}{2}+\frac{\delta^2}{4}+(\gamma_e\theta)^2}(1-\Delta)$$

Δ = electron recoil term < 3%

$$a_0 \equiv 2.15\frac{\lambda_L}{w_0}\sqrt{\frac{U}{\sigma_t}}$$

= laser parameter (dimensionless amplitude of the vector potential associated to the laser e.m. field)

Typical laser parameters:

– angle $\delta \approx 7^o \rightarrow 1+\cos\delta \approx 2+10^{-6}$, $\delta^2/4 \approx 0.004$

– wavelength λ_L=0.5μm, focal spot w_0=25μm, pulse energy U=0.5J, pulse time σ_t=1.5ps → $a_0^2 \approx 2.5\cdot10^{-3}$

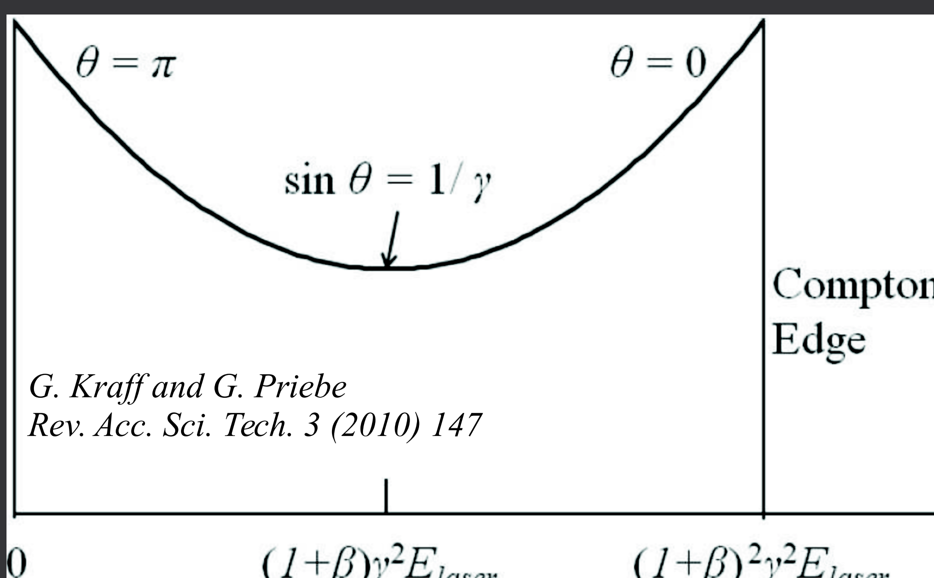

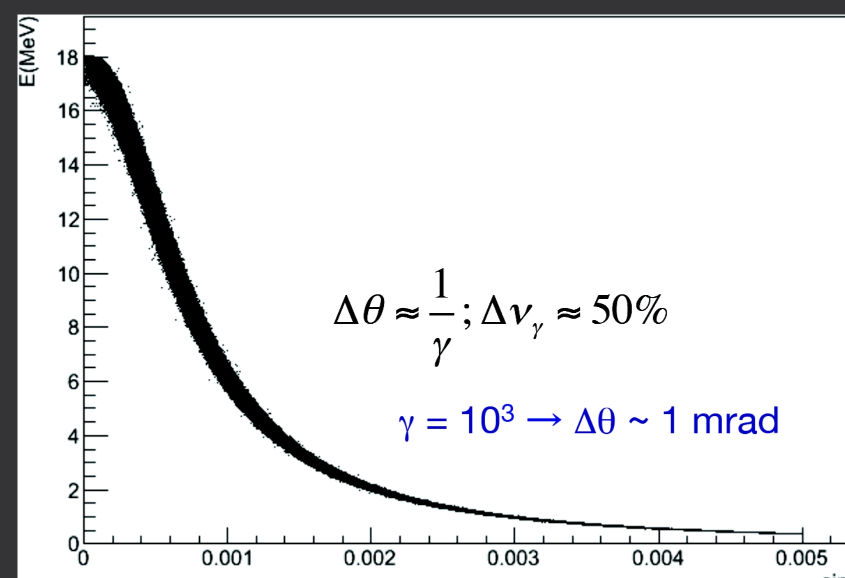

Inverse Compton Scattering at ELI-NP

O. Adriani et al., arXiv:1407.3669 (2014)

$$E_\gamma = 2\gamma_e^2 E_L \frac{1+\cos\delta}{1+\frac{a_0^2}{2}+\frac{\delta^2}{4}+(\gamma_e\theta)^2}(1-\Delta)$$

Maximum energy E_γ^{max} set by varying the electron beam kinetic energy T_e:

$$E_\gamma^{max} \approx 9.55\, eV \cdot \gamma_e^2, \quad \gamma_e = 1 + T_e/mc^2$$

Minimum γ energy set by collimation, using the strong (E,θ) correlation

Inverse Compton Scattering at ELI-NP

O. Adriani et al., arXiv:1407.3669 (2014)

$$E_\gamma = 2\gamma_e^2 E_L \frac{1+\cos\delta}{1+\frac{a_0^2}{2}+\frac{\delta^2}{4}+(\gamma_e\theta)^2}(1-\Delta)$$

Maximum energy E_γ^{max} set by varying the electron beam kinetic energy T_e:

$$E_\gamma^{max} \approx 9.55\, eV \cdot \gamma_e^{2,} \quad \gamma_e = 1 + T_e / mc^2$$

Minimum γ energy set by collimation, using the strong (E,θ) correlation

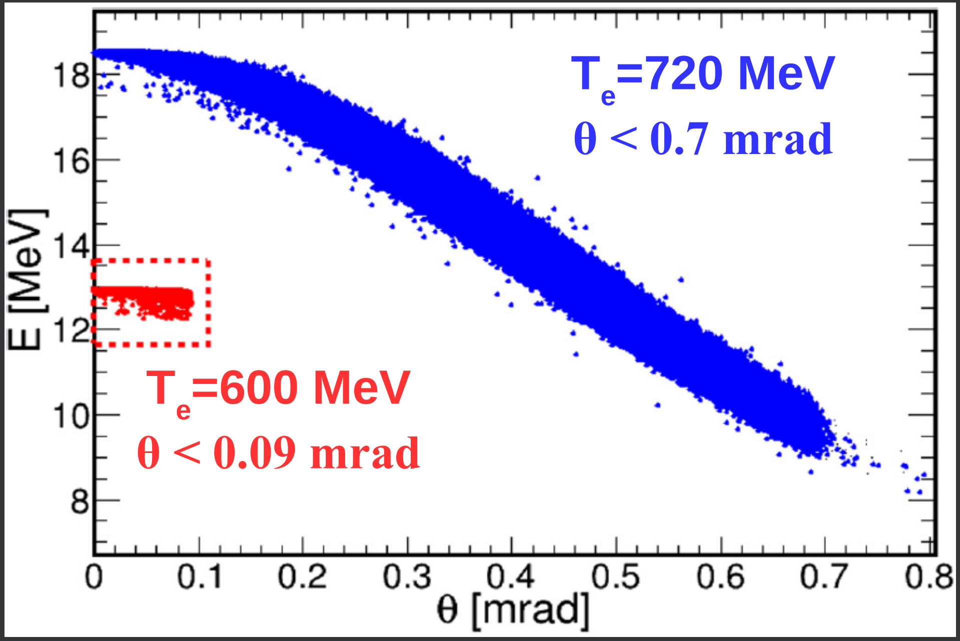

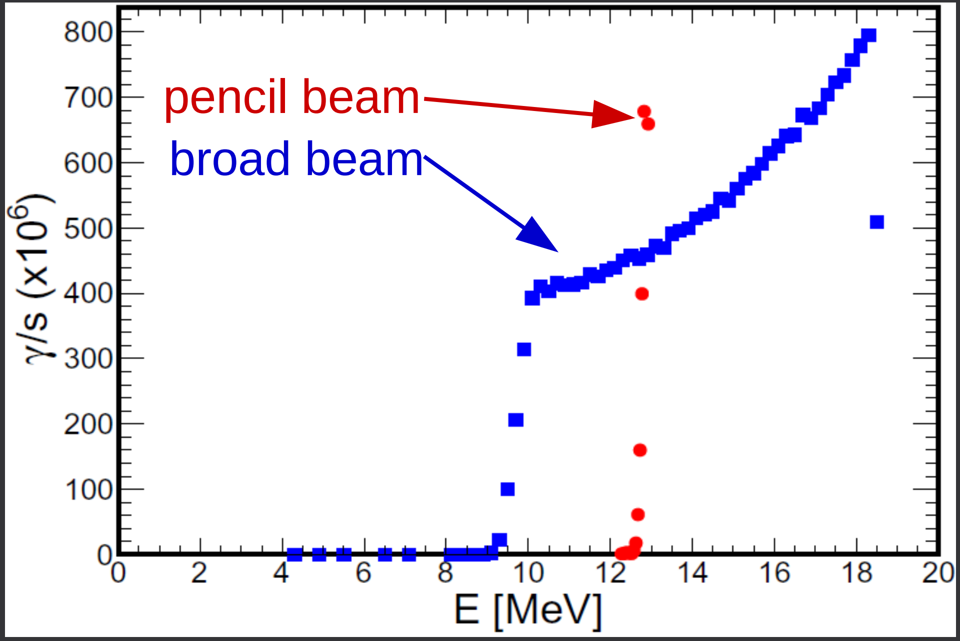

Inverse Compton Scattering at ELI-NP

Energy resolution:

$$\left(\frac{\Delta E_\gamma}{E_\gamma}\right)^2 \approx \underbrace{(\gamma_e \theta_{col})^2}_{\text{collimate } \sim 10^{-5}\text{rad}} + \underbrace{4\left(\frac{\Delta \gamma_e}{\gamma_e}\right)^2}_{\text{electron energy spread } \sim 0.1\%} + \underbrace{\left(\frac{\Delta \nu_L}{\nu_L}\right)^2}_{\text{laser band width } \sim 0.1\%} + \underbrace{\left(\frac{\epsilon_n}{\sigma}\right)^2}_{\text{collision point}}$$

$\varepsilon_n \approx 0.4$ mm·mrad (rms normalized transverse emittance); σ = collision spot size

Inverse Compton Scattering at ELI-NP

Energy resolution:

$$\left(\frac{\Delta E_\gamma}{E_\gamma}\right)^2 \approx (\gamma_e \theta_{col})^2 + 4\left(\frac{\Delta \gamma_e}{\gamma_e}\right)^2 + \left(\frac{\Delta \nu_L}{\nu_L}\right)^2 + \left(\frac{\epsilon_n}{\sigma}\right)^2$$

- collimate ~10^{-5}rad
- electron energy spread ~0.1%
- laser band width ~0.1%
- collision point

$\varepsilon_n \approx 0.4$ mm·mrad (rms normalized transverse emittance); σ = collision spot size

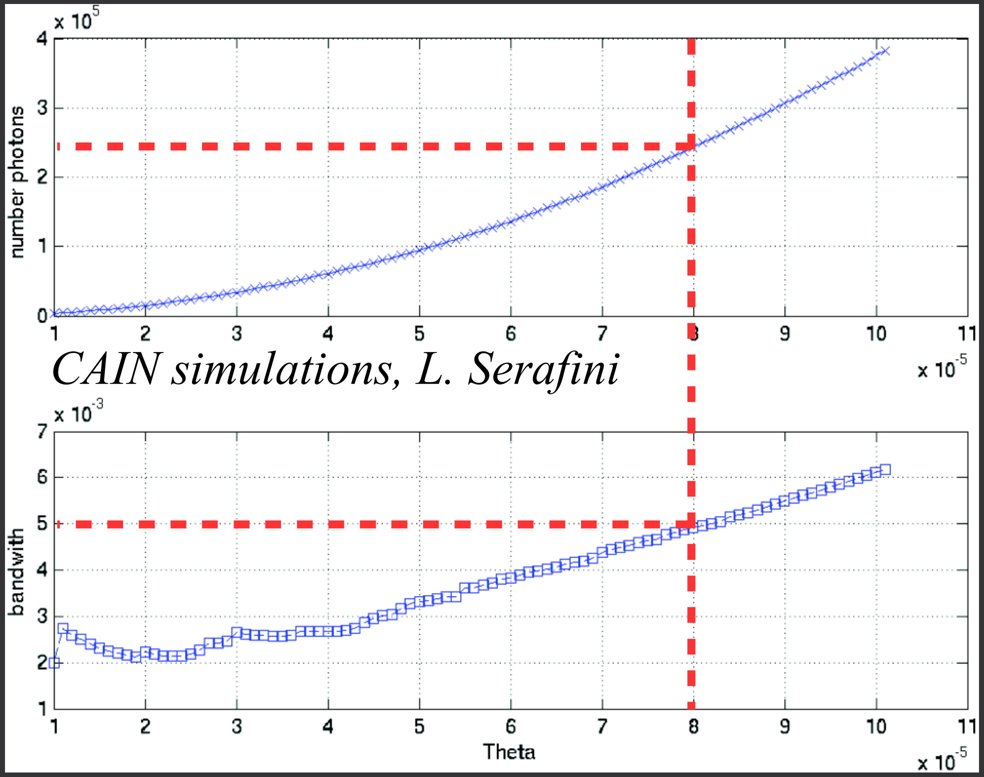

Inverse Compton Scattering at ELI-NP

Energy resolution:

$$\left(\frac{\Delta E_\gamma}{E_\gamma}\right)^2 \approx (\gamma_e \theta_{col})^2 + 4\left(\frac{\Delta \gamma_e}{\gamma_e}\right)^2 + \left(\frac{\Delta \nu_L}{\nu_L}\right)^2 + \left(\frac{\epsilon_n}{\sigma}\right)^2$$

- collimate ~10^{-5}rad
- electron energy spread ~0.1%
- laser band width ~0.1%
- collision point

$\varepsilon_n \approx 0.4$ mm·mrad (rms normalized transverse emittance); σ = collision spot size

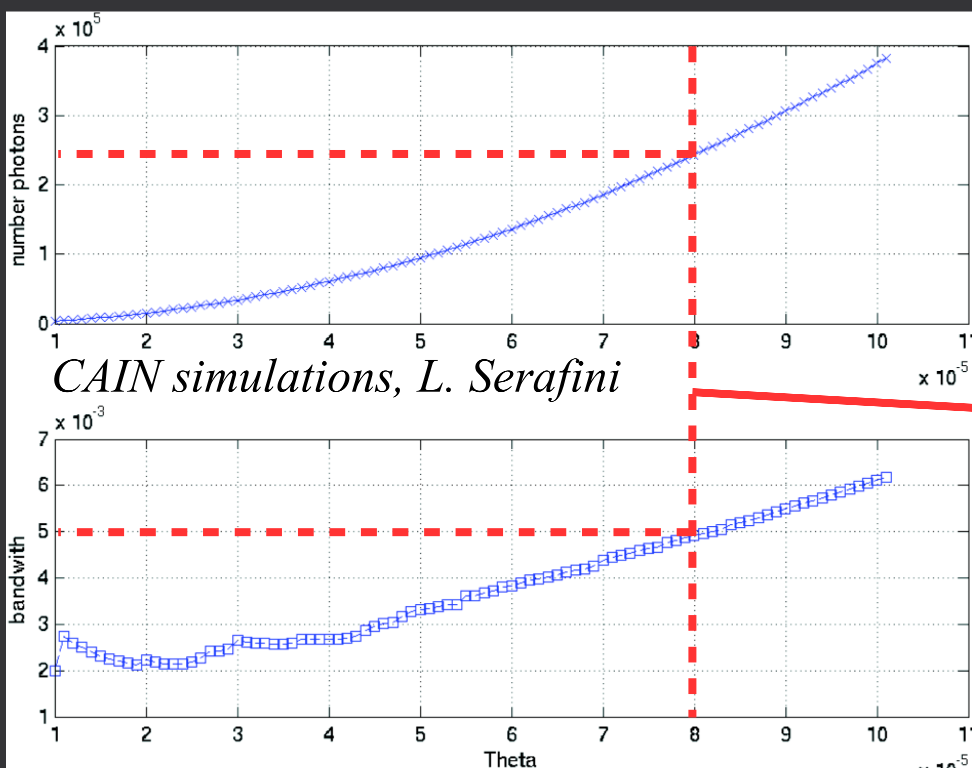

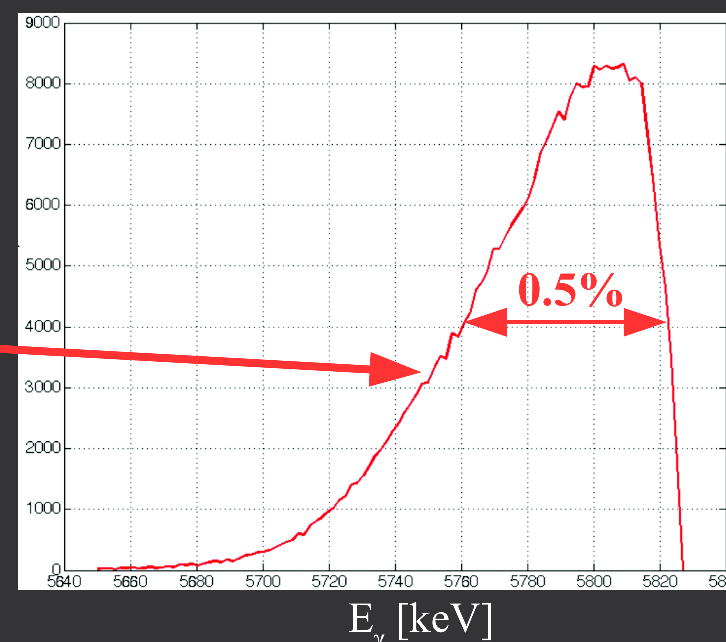

Trade-offs can be made between beam focusing, energy resolution and beam intensity.

Inverse Compton Scattering at ELI-NP

$$P_\gamma \approx \left(1-\frac{3}{2}\Delta^2\right)\left(1-\frac{\gamma^2\theta^2}{2}\right) \Rightarrow P_\gamma > 0.995\, P_{laser}$$

Laser beam polarization is transferred to the gamma beam (no need for polarized electron beam).
Small corrections exist: $P_\gamma \approx 99\%$

outgoing photon $\langle \xi'_x \rangle$ for
an incoming photon with ε=2.4eV
and 100% liniar polarization along x
and an incoming electron with E_e=720MeV along z
→ **polarization > 99%** for forward scattered γ at $\varepsilon'_\gamma \approx$19MeV

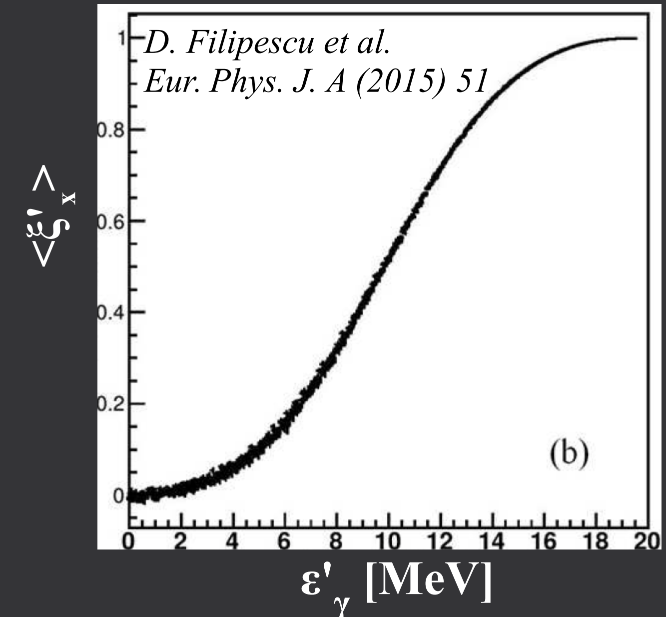

Inverse Compton Scattering at ELI-NP

$$P_\gamma \approx \left(1-\frac{3}{2}\Delta^2\right)\left(1-\frac{\gamma^2\theta^2}{2}\right) \Rightarrow P_\gamma > 0.995\, P_{laser}$$

Laser beam polarization is transferred to the gamma beam (no need for polarized electron beam).
Small corrections exist: $P_\gamma \approx 99\%$

outgoing photon $<\xi'_x>$ for
an incoming photon with $\varepsilon = 2.4$eV
and 100% liniar polarization along x
and an incoming electron with $E_e = 720$MeV along z
→ **polarization > 99%** for forward scattered γ at $\varepsilon'_\gamma \approx 19$MeV

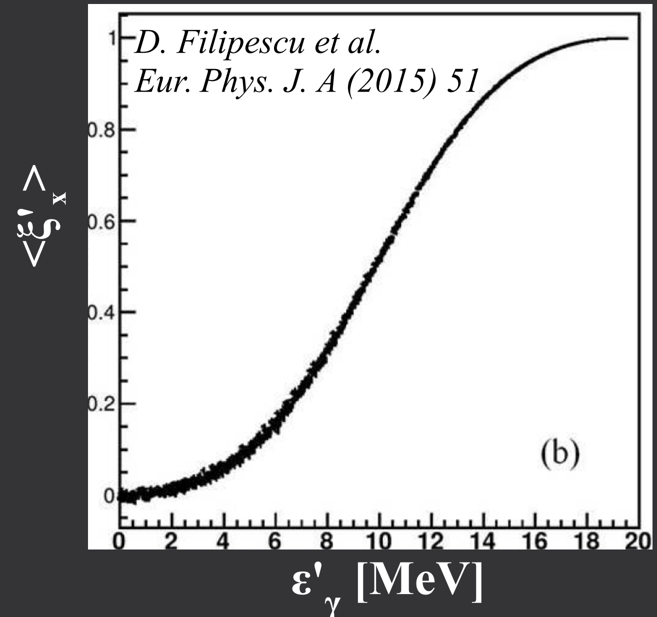

Luminosity: $$L = \frac{N_L N_e f}{4\pi\sigma^2} = \frac{1.3\cdot 10^{18}\cdot 1.6\cdot 10^{9}\cdot 3200\, s^{-1}}{4\pi\cdot(15\mu m)^2} = 2.5\cdot 10^{35}\, cm^{-2} s^{-1}$$

f = bunch crossing frequency   σ = collision spot size

$$\sigma_{Thomson} = \frac{8\pi}{3} r_e^2 = 0.67\, b \quad \Rightarrow \quad N_\gamma = L\cdot\sigma \approx 10^{11}\, s^{-1}$$

At LHC: $L \approx 10^{34} cm^{-2} s^{-1}$. Spectral luminosity ($L/\Delta E$), spectral density ($N_\gamma/\Delta E$), brilliance B

Inverse Compton Scattering at ELI-NP

$$P_\gamma \approx \left(1-\frac{3}{2}\Delta^2\right)\left(1-\frac{\gamma^2\theta^2}{2}\right) \Rightarrow P_\gamma > 0.995\,P_{laser}$$

Laser beam polarization is transferred to the gamma beam (no need for polarized electron beam). Small corrections exist: $P_\gamma \approx 99\%$

outgoing photon $\langle \xi'_x \rangle$ for
an incoming photon with ε=2.4eV
and 100% liniar polarization along x
and an incoming electron with E_e=720MeV along z
→ **polarization > 99%** for forward scattered γ at $\varepsilon'_\gamma \approx$19MeV

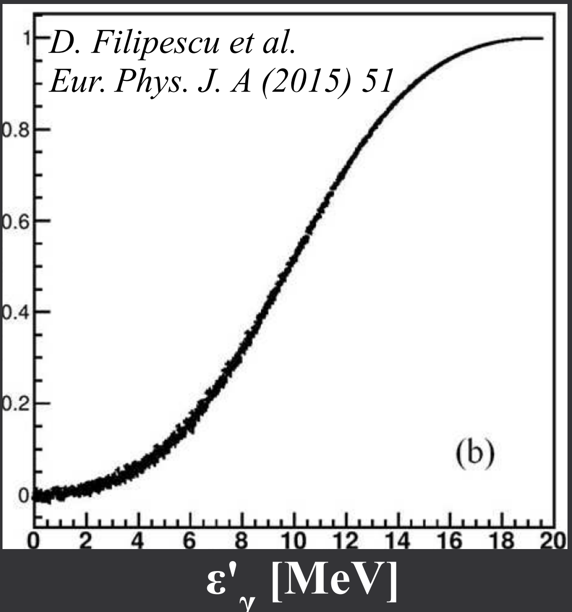

Luminosity: $$L = \frac{N_L N_e f}{4\pi\sigma^2} = \frac{1.3\cdot10^{18}\cdot1.6\cdot10^{9}\cdot3200\,s^{-1}}{4\pi\cdot(15\,\mu m)^2} = 2.5\cdot10^{35}\,cm^{-2}s^{-1}$$

f = bunch crossing frequency σ = collision spot size

$$\sigma_{Thomson} = \frac{8\pi}{3} r_e^2 = 0.67\,b \quad\Rightarrow\quad N_\gamma = L\cdot\sigma \approx 10^{11}\,s^{-1}$$

At LHC: $L \approx 10^{34} cm^{-2}s^{-1}$. Spectral luminosity (L/ΔE), spectral density (N_γ/ΔE), brilliance B

Time structure of the beam:
- macro-bunch frequency = 100Hz
- macro-bunch structure = 32 bunches of 1-2ps at 16ns apart → duration = 0.5µs
- due to special collision technique

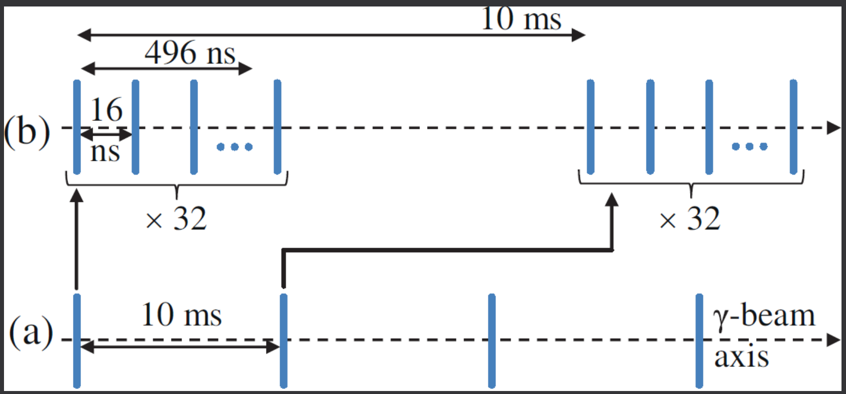

ELI-NP Gamma Beam Systems

laser rep. rate 100Hz → “dragon-shaped” **laser recirculation system at IP**

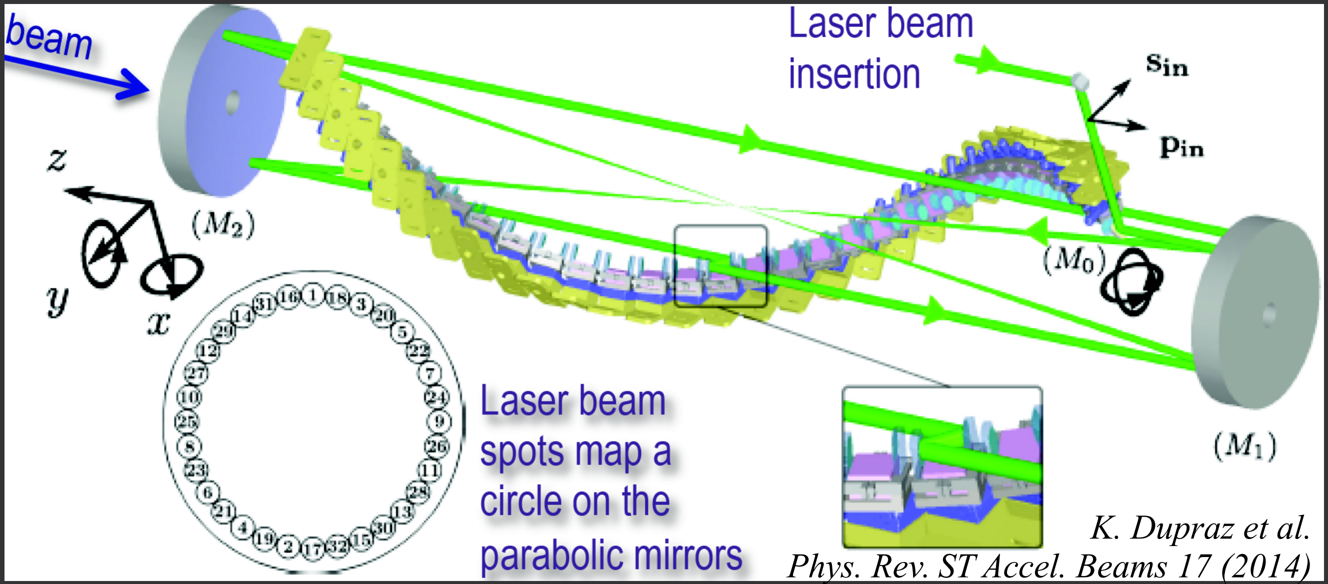

K. Dupraz et al.
Phys. Rev. ST Accel. Beams 17 (2014)

ELI-NP Gamma Beam Systems

laser rep. rate 100Hz → "dragon-shaped" **laser recirculation system at IP**

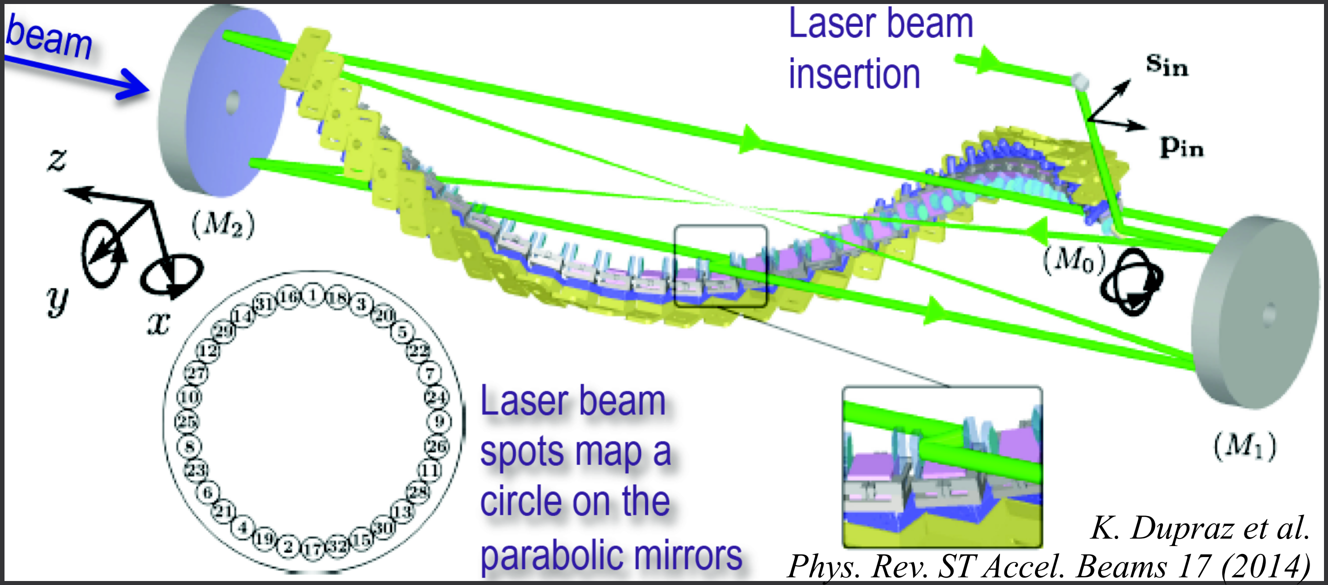

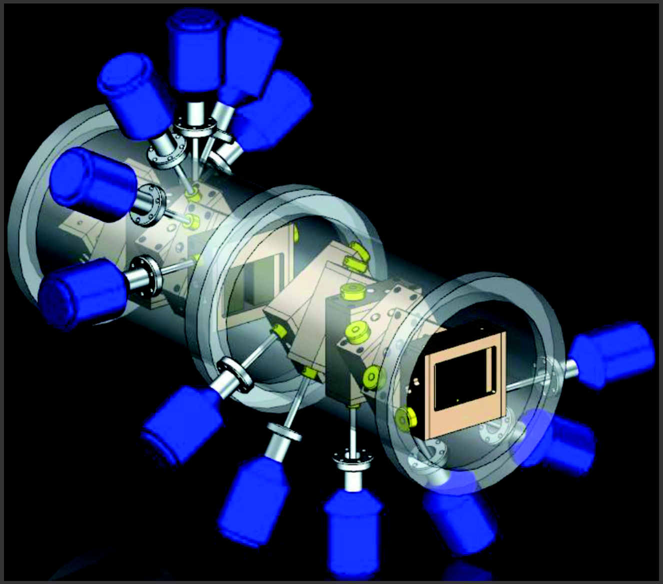

Gamma **beam collimation system**:

– low gamma transmission: tungsten 2cm thick
– adjustable aperture (BW): continuously in 1-20mm
– avoid beam contamination (radiation): 14 slits at 25.7°

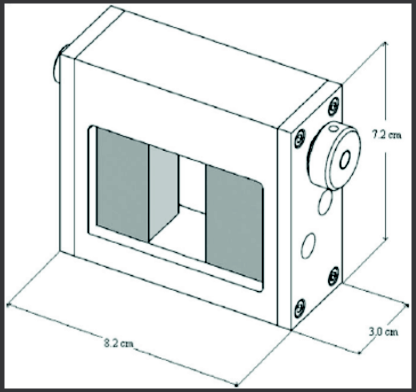

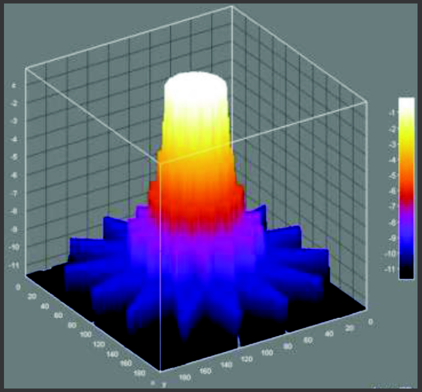

Inverse Compton Scattering at ELI-NP

Photon inverse scattering on ultra-relativistic electrons:
– most powerful frequency amplifier: eV → MeV
– high energy resolution: ~0.5% (but 0.3% reachable)
– strong forward focusing: divergence ~ 0.1 mrad
– strong (E,θ) correlation: hardening via collimation
– almost complete linear polarization: >99%
– high intensity 10^{12} γ/s, spectral density 10^{5} γ/s/eV, brilliance 10^{20}-10^{23} γ/(s·mrad^{2}·mm^{2}·0.1%BW)
→ we have a real **photon accelerator**

Inverse Compton Scattering at ELI-NP

Photon inverse scattering on ultra-relativistic electrons:
– most powerful frequency amplifier: eV → MeV
– high energy resolution: ~0.5% (but 0.3% reachable)
– strong forward focusing: divergence ~ 0.1 mrad
– strong (E,θ) correlation: hardening via collimation
– almost complete linear polarization: >99%
– high intensity 10^{12} γ/s, spectral density 10^5 γ/s/eV, brilliance 10^{20}-10^{23} γ/(s·mrad²·mm²·0.1%BW)
→ we have a real **photon accelerator**

Energy (MeV)	0.2 – 19.5
Spectral Density (ph/s·eV)	> $0.5\cdot10^4$
Bandwidth rms (%)	≤ 0.5
# photons per pulse within FWHM bdw.	~10^5
# photons/s within FWHM bdw.	10^8 – 10^9
Source rms size (μm)	10 – 30
Source rms divergence (μrad)	25 – 200
Peak brilliance (N_{ph}/sec·mm²·mrad²·0.1%)	10^{20} – 10^{23}
Radiation pulse length rms (ps)	0.7 – 1.5
Linear polarization (%)	> 95
Macro repetition rate (Hz)	100
# pulses per macropulse	32
Pulse–to–pulse separation (nsec)	16

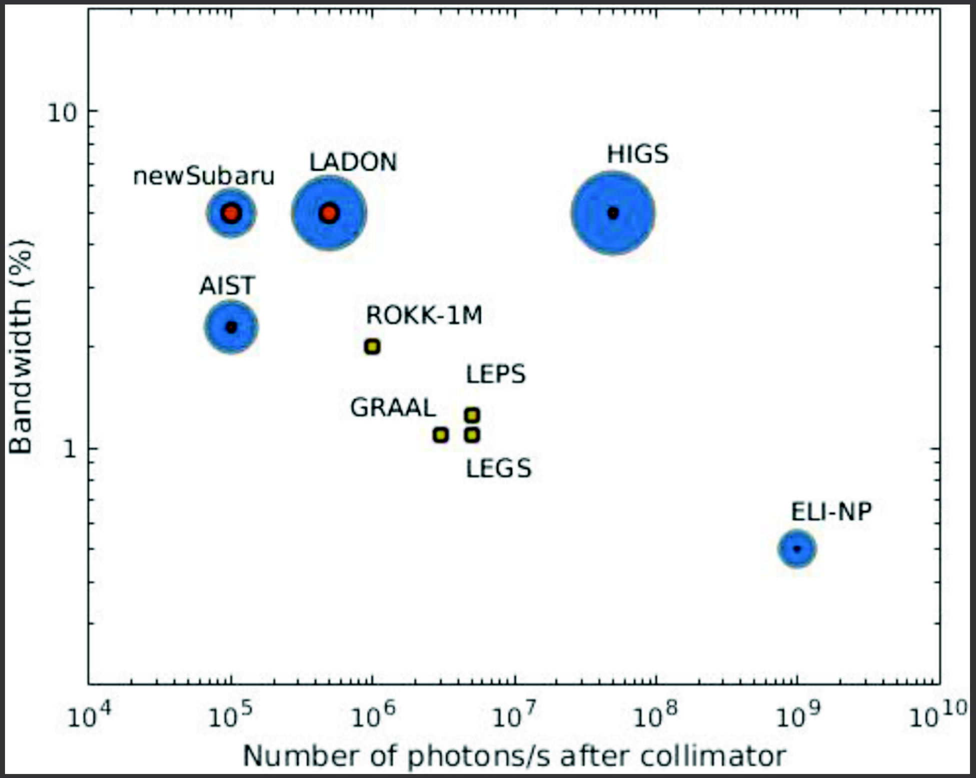

Inverse Compton Scattering at HIGS

H.R. Weller et al., Prog. Part. Nucl. Phys. 62 (2009) 257

Parameters of major Compton gamma source facilities around the world

Project name	LADON[a]	LEGS	ROKK-1M[b]	GRAAL	LEPS	HIγS[c]
Location	Frascati Italy	Brookhaven US	Novosibirsk Russia	Grenoble France	Harima Japan	Durham US
Storage ring	Adone	NSLS	VEPP-4M	ESRF	SPring-8	Duke-SR
Electron energy (GeV)	1.5	2.5–2.8	1.4–6.0	6	8	0.24–1.2
Laser energy (eV)	2.45	2.41–4.68	1.17–4.68	2.41–3.53	2.41–4.68	1.17–6.53
γ-beam energy (MeV)	5–80	110–450	100–1600	550–1500	1500–2400	1–100 (158)[d]
Energy selection	Internal tagging	External tagging	(Int or Ext?) tagging	Internal tagging	Internal tagging	Collimation
γ-energy resolution (FWHM)						
ΔE (MeV)	2–4	5	10–20	16	30	0.008–8.5
$\frac{\Delta E}{E}$ (%)	5	1.1	1–3	1.1	1.25	0.8–10
E-beam current (A)	0.1	0.2	0.1	0.2	0.1–0.2	0.01–0.1
Max on-target flux (γ/s)	5×10^5	5×10^6	10^6	3×10^6	5×10^6	10^4–5×10^8
Max total flux (γ/s)						10^6–3×10^9[e]
Years of operation	1978–1993	1987–2006	1993–	1995–	1998–	1996–

Inverse Compton Scattering at HIGS

H.R. Weller et al., Prog. Part. Nucl. Phys. 62 (2009) 257

Parameters of major Compton gamma source facilities around the world

Project name	LADON[a]	LEGS	ROKK-1M[b]	GRAAL	LEPS	HIγS[c]
Location	Frascati Italy	Brookhaven US	Novosibirsk Russia	Grenoble France	Harima Japan	Durham US
Storage ring	Adone	NSLS	VEPP-4M	ESRF	SPring-8	Duke-SR
Electron energy (GeV)	1.5	2.5–2.8	1.4–6.0	6	8	0.24–1.2
Laser energy (eV)	2.45	2.41–4.68	1.17–4.68	2.41–3.53	2.41–4.68	1.17–6.53
γ-beam energy (MeV)	5–80	110–450	100–1600	550–1500	1500–2400	1–100 (158)[d]
Energy selection	Internal tagging	External tagging	(Int or Ext?) tagging	Internal tagging	Internal tagging	Collimation
γ-energy resolution (FWHM)						
ΔE (MeV)	2–4	5	10–20	16	30	0.008–8.5
$\frac{\Delta E}{E}$ (%)	5	1.1	1–3	1.1	1.25	0.8–10
E-beam current (A)	0.1	0.2	0.1	0.2	0.1–0.2	0.01–0.1
Max on-target flux (γ/s)	5×10^5	5×10^6	10^6	3×10^6	5×10^6	10^4–5×10^8
Max total flux (γ/s)						10^6–3×10^9[e]
Years of operation	1978–1993	1987–2006	1993–	1995–	1998–	1996–

HIGS @ TUNL/Duke
current state-of-the-art

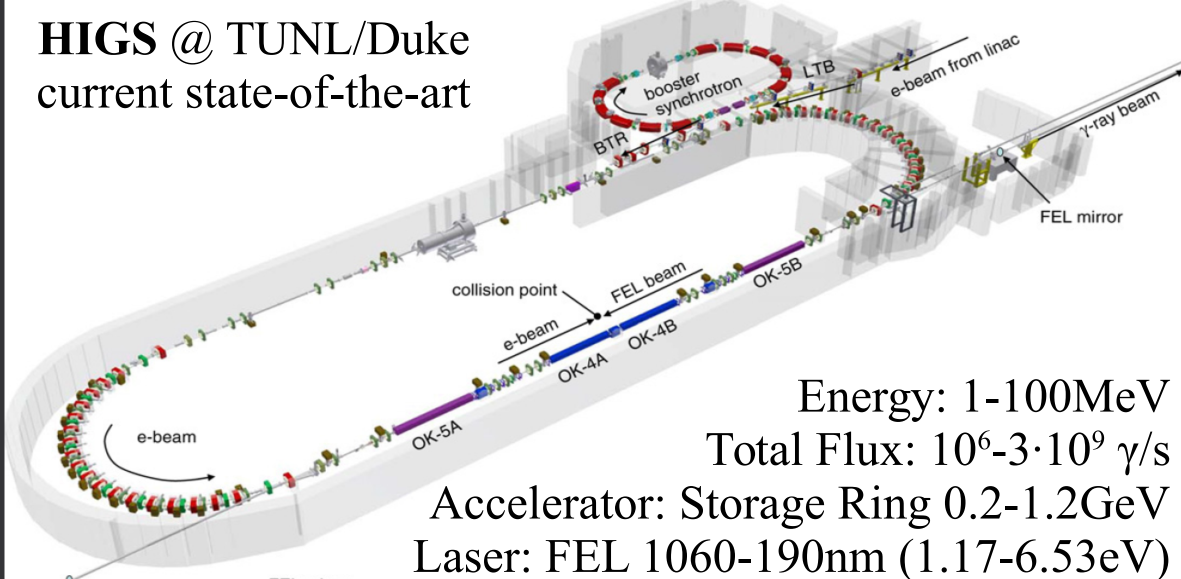

Energy: 1-100MeV
Total Flux: 10^6-$3\cdot10^9$ γ/s
Accelerator: Storage Ring 0.2-1.2GeV
Laser: FEL 1060-190nm (1.17-6.53eV)

	SD γ/s/eV	BW %	spot	bunch cross.	P %
HIGS	10^2	3	cm	MHz	99
ELI-NP	10^4	0.5	mm	kHz	99

Vast research program:
– NRF (^{138}Ba, ^{88}Sr, ^{92}Zr, ^{94}Mo, ^{40}Ar)
– nuclear astrophysics
– γ–^{3}He/^{4}He photodisintegration
– national security applications

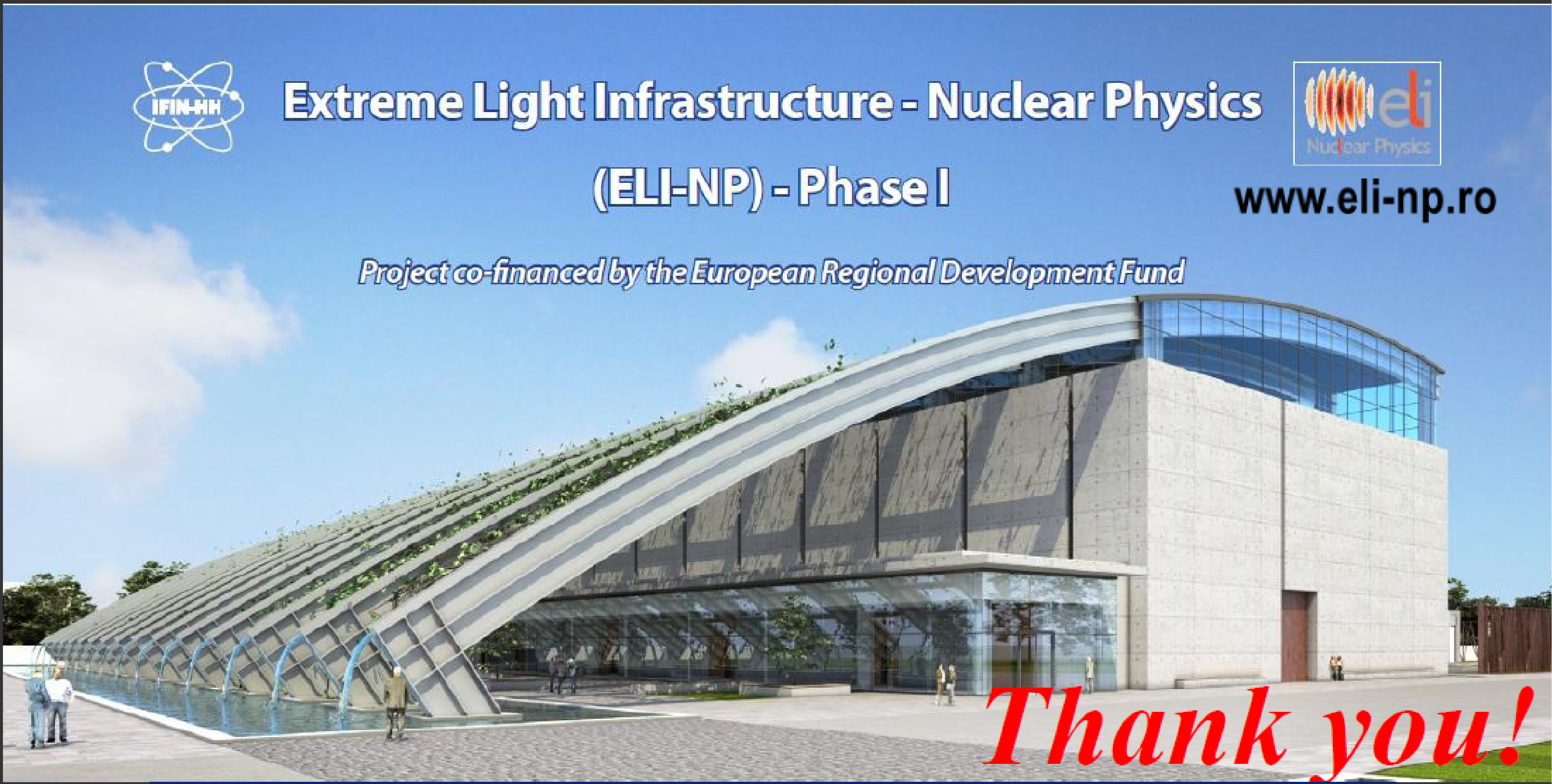
Extreme Light Infrastructure - Nuclear Physics
(ELI-NP) - Phase I
www.eli-np.ro
Project co-financed by the European Regional Development Fund
Thank you!